DYNAMICS OF CLASSICAL YANG MILLS FIELDS COUPLED TO HIGGS FIELD

by

Berç Deruni

Submitted to Graduate School of Natural and Applied Sciences

in Partial Fulfillment of the Requirements

for the Degree of Doctor of Philosophy in

Physics

Yeditepe University

2019

DYNAMICS OF CLASSICAL YANG MILLS FIELDS COUPLED TO HIGGS FIELD

APPROVED BY:

Prof. Dr. Avadis Simon Hacınlıyan ..... 
(Thesis Supervisor)
(Yeditepe University)

Prof. Dr. Ertan Akşahin ..... 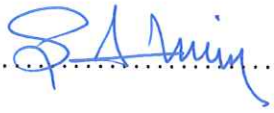
(Yeditepe University)

Prof. Dr. Şerife İpek Karaaslan ..... 
(Yeditepe University)

Prof. Dr. Yani Skarlatos ..... 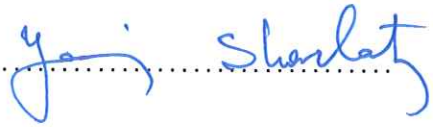
(Boğaziçi University)

Assist. Prof. Dr. Nazım Ziya Perdahçı ..... 
(Mimar Sinan University)

DATE OF APPROVAL: ..../..../2019

To my father...

ACKNOWLEDGEMENTS

I would like to thank to my supervisor, Prof. Avadis Hacınlıyan for giving his time and interest during the thesis. Without his guidance it would become rather difficult to finish this work.

I would like to thank to my family and friends who supported me during the thesis work.

ABSTRACT

DYNAMICS OF CLASSICAL YANG MILLS FIELDS COUPLED TO HIGGS FIELD

Classical Yang Mills fields are analyzed in the context of nonlinear dynamical systems. Although the theory is described by complicated set of coupled partial differential equations, under specific ansatzes it is possible to obtain simpler dynamical system whose equations of motion can be represented by coupled ordinary differential equations. It is numerically shown that the reduced system possesses chaotic behaviour. On the other hand, the coupling of Higgs field stabilizes chaotic behavior of Yang Mills fields. This stabilization can be attributed to the additional harmonic oscillator part appearing in the Hamiltonian. It is numerically verified that the coefficient of harmonic oscillator term dramatically changes the behavior of the system corresponding to two different Yang-Mills-Higgs systems. For fixed energy, a small increase in the coefficient suppresses the chaos and the system is dominated with quasiperiodic and periodic solutions. Even if the reduced mechanical systems are simpler than the original ones, still it is not possible to express the solutions with elementary functions. But using perturbation theory one can make good prediction for dynamics of the system. For this purpose, Lie Transform perturbation theory is used which is a very efficient tool especially for Hamiltonian systems. With the implemented algorithm approximate integrals are constructed beside the normalized solutions. Those solutions and integrals are expressed as a series, and they are used to simulate the mechanical system. Although the convergence of series is not guaranteed they turn out to be in good agreement with the numerical results, especially for the periodic and quasiperiodic regimes.

ÖZET

KLASİK YANG MİLLS HİGGS ALANLARININ DİNAMİĞİ

Klasik Yang Mills alanları lineer olmayan dinamik sistemler öğesinde incelenmiştir. Teorinin karmaşık kismi diferansiyel denklem setlerinden oluşmasına karşın, bazı özel durumlarda bu denklemlerden basit bir dinamik sistem elde etmek mümkün, ve bu sistemin hareket denklemleri sıradan diferansiyel denklemlerle tarif edilebilir. Nümerik olarak yapılan araştırmalar sonucunda Yang Mills alanlarından elde edilen indirgenmiş sistemde kaosun varlığı saptanmıtır. Öte yandan Yang Mills alanlarına bağlanan Higgs alanı, kaosu stabilize etmektedir. Higgs alanın kaosu stabilize etmesindeki temel etken, Higgs alanının sistemin enerji denkleminde oluşturduğu harmonik salınıcı terimidir. Nümerik olarak görülmüştür ki bu terimin katsayısı değiştirildiğinde sistemin davranışında ani bir değişim meydana gelmektedir. Öyle ki sabit bir enerjide bu katsayıdaki küçük bir artışın sistemdeki kaosu bastırdığı gibi periyodik ve periyodiğe yakın hareketler meydana getirmektedir. Yang Mills alanlarından elde edilen indirgenmiş sistem her ne kadar basit olsa da, çözümlerini sıradan fonksiyonlarla belirtmek mümkün değildir. Fakat pertürbasyon teorisi kullanılarak sistemin hareketi ile ilgili tahminler yapmak mümkündür. Bu amaçla Lie Dönüşüm pertürbasyon teorisi kullanılmıştır ki bu araç özellikle enerji korunumlu sistemler için idealdir. Uygulanan algoritma ile normalize edilmiş çözümlerin yanı sıra yaklaşık integraller bulunmuştur. Bu çözümler ve integraller seri açılımı ile ifade edilmiştir ve incelediğimiz sistemin simülasyonunda kullanılmıştır. Seri ifadelerin yakınsaklığının garantisi olmamasına rağmen, özellikle sistemde periyodik ve periyodiğe yakın hareketlerin hakim olduğu durumlarda nümerik sonuçlarla uyumlu neticeler elde edilmiştir.

TABLE OF CONTENTS

LIST OF FIGURES

LIST OF SYMBOLS/ABBREVIATIONS

α	Parameter representing coefficient of quartic term
β	Scaling parameter
Ω	Relative phase
μ	Space-time index
ν	Space-time index
ε_{ijk}	Levi-Civita symbol
ε	Small perturbation parameter
θ_i	i^{th} angle
λ	Scaling parameter
ϕ	Higgs field
$a_{m_1 m_2}$	Coefficients of resonant terms
A	Magnitude of periodic function
A^a_μ	SU(2) gauge potential
D_μ	Covariant derivative
$F^a_{\mu\nu}$	SU(2) field strength tensor
E	Energy
g	Parameter representing coefficient of harmonic oscillator term
g_i	Generating functions
H	Hamiltonian
I_n	Integral expression
J	Action angle variables
K	Normalized hamiltonian
L	Lagrangian function
L_i	i^{th} Lyapunov exponent
$L_S f$	Lie Derivative of f along S
$\mathbb{M}^{2n}$	2n-Dimensional manifold
M_g	Transformation introduced by Dragt and Finn

p	Parameter representing coefficient of Higgs Field
p_i	i^{th} Momentum variable
P	New momentum variable after canonical transformation
q	Position variable
P	New position variable after canonical transformation
t	Time
T^b	Generators of SU(2) algebra
v	Magnitude of Higgs Field
V	Potential function
x	Position variable
y	Position variable

1. INTRODUCTION

In recent years there has been much attention on the dynamics of Yang Mills theories, which belong to nonabelian gauge theories, and they play important role in the construction of the standard model of particle physics. This has been a primer to understanding of chaotic dynamics in field theories. The study originally grew out with an aim of understanding the structure of the field-theoretic vacuum and the asymptotic states of the theory with reference to strong interaction physics. This was motivated by the belief that there was a connection between color confinement and chaos in quantum chromodynamics. Further interest in such investigations arose because some gauge theories support solitons, and these non-trivial topological structures[1] and chaos are examples of opposite extremes in nonlinear dynamics, so their coexistence needs to be understood[2].

The systems considered are simplified version for the classical limits of SU(2) Yang Mills theory, assuming the gauge fields are time dependent and spatially homogeneous. This choice reduces the degrees of freedom in the theory and yield a dynamical system whose equation of motions are governed by coupled ordinary differential equations. By this way one simplifies the complicated set of partial differential equations described by the theory.

It has been verified that pure SU(2) Yang Mills fields possesses chaotic nature, especially using numerical methods namely Lyapunov exponent[3] and Poincaré sections. Analytical methods also support this result. In terms of Liouville integrability[4] there should be two constants of motion, but in the dynamics of Yang Mills fields only Hamiltonian is conserved, and the system does not have an additional first integral[5, 6].

On the other hand, extensive investigations has been made on stabilizing mechanisms on Yang Mills fields. Numbers of field theoretical and topological models described for this purpose but the most prominent has been the Higgs mechanism. The Yang-Mills-Higgs system has much significance in the theory of particle physics, since the theory incorporates spontaneous symmetry breaking[7], and has been successfully applied for the unification of the fundamental forces in nature. It appears that addition of Higgs term exhibits chaos order

transitions for specific values of parameter and regular motion becomes dominant.

Since the systems under investigation are non-linear dynamical systems reduced by using special ansatz, detailed study can be made using the theory of non-linear dynamics in order to obtain qualitative information about the system such as equilibrium solutions, stability and non-stability of these solutions, bifurcation curves, periodic and chaotic solutions, and so on[8, 9]. However in many cases the procedure is complex to carry out without making some reductions. One way to simplify the analysis is localization. Instead of considering the whole phase space, one chooses a small neighborhood of special points and then carry out the analysis to determine the behavior of the system at these points. One another method is perturbation theory[10]. One can bring the system more amenable or put it simpler form (normal form) with suitable coordinate transformation. There have been variety of approaches to do so, starting from the pioneering work of Poincaré[11]. In the case of Hamiltonian[12] systems the procedure is exploited with Birkhoff-Gustavson[13, 14] normalization, which is originally implemented for the perturbed harmonic oscillator. Further improvements have been made with the Lie Transform method. The method uses Lie algebraical relations to reduce the system to simpler form step by step. The approach becomes more popular for its practical implementation, and it provides better understanding on the algebraic and geometric structure of the Hamiltonian systems.

The results obtained from the normalized system is also valid for the original system since they are connected with a near identity coordinate transformation. However, the expressions for the normalized system usually do not converge, this is the case expected when dealing with non-integrable systems. Hopefully one can get meaningful information without going to higher orders of normalization and there is an optimal order of normalization where the original system can be reproduced with high accuracy[15]. The motivation behind this results comes from the famous perturbation theory for Hamiltonian systems known as KAM[16, 17] theorem which states that perturbed integrable systems have qualitatively the same dynamics with the unperturbed ones, namely quasi-periodic motions are retained in the phase space.

The aim of the study is to obtain analytical results using classical perturbation to describe the dynamical system resulting from SU(2) Yang-Mills-Higgs system, and comparing them with numerical methods. Representing the system with normal forms as far as chaos starts to exhibit, gives better understanding on the effect of Higgs term introduced, and on the route of chaos order transitions.

2. CLASSICAL YANG-MILLS FIELDS

Today's modern description of the elementary particles and their interactions are based on gauge theory. The developments of the gauge theories have their roots in quantum mechanics where the principle of the gauge invariance was discovered. The principle become apparent when Yang and Mills introduced the first nonabelian gauge theory in 1954.Then gauge theories began to describe all known fundamental interactions, from electromagnetism, weak interactions to the strong interactions and even gravity.
In this study we consider Yang-Mills fields in 3+1 dimensional Minkowski space-time with internal degrees of freedom respecting an SU(2) symmetry. The equations of motion are

$$\partial^{\mu} F_{\mu\nu} + g\epsilon^{abc} A^{a\mu} F^{c}_{\mu\nu} = 0 \tag{2.1}$$

where

$$F^{a}_{\mu\nu} = \partial_{\mu} A^{a}_{\nu} - \partial_{\nu} A^{a}_{\mu} + g\epsilon^{abc} A^{b}_{\mu} A^{c}_{\nu} \tag{2.2}$$

is the field strength tensor, A^{a}_{μ} is the vector potential and g is the coupling constant. The latin indices a, b, c correspond to internal degrees of freedom and take the values of $1, 2, 3$ while Greek indices correspond to spacetime components taking values $0, 1, 2, 3$.
The procedure to study dynamical systems require the reduction of partial differential equations to ordinary differential equations. This reduction is done by the assumption that the gauge potentials are only time dependent and homogenous in space coordinates i.e

$$A^{a}_{\mu} = A^{a}_{\mu}(t) \tag{2.3}$$

Using this condition and fixing the gauge by $A^{a}_{0} = 0$ eq(2.1) can be written as

$$\ddot{A}^{a}_{i} - g^{2}(A^{a}_{j} A^{b}_{j} A^{b}_{i} - A^{b}_{j} A^{b}_{j} A^{a}_{i}) = 0 \tag{2.4}$$

2.1. CHAOS IN HOMOGENEOUS YANG-MILLS FIELDS

In order to expect chaotic behavior in a dynamical system it must include at least two degrees of freedom. Using $x = gA_1^1$ and $y = gA_2^2$ as two nonzero gauge potential components the system is reduced to mechanical system having non-linear coupling with two degrees of freedom. The equations of motion are

$$\ddot{x} + xy^2 = 0, \quad \ddot{y} + x^2 y = 0 \tag{2.5}$$

with the following Hamiltonian

$$H = \frac{1}{2}\dot{x}^2 + \frac{1}{2}\dot{y}^2 + \frac{1}{2}x^2y^2 \tag{2.6}$$

The system describes oscillators coupled with quartic x^2y^2 potential. Despite its simplicity the system is non-integrable and exhibits chaotic dynamics. For numerical investigation of this chaoticity, Lyapunov characteristic exponents are calculated with the Fortran program which uses Wolf Algorithm[3].The exponents are plotted up to a timescale of 1000 which is shown in Figure 2.1.

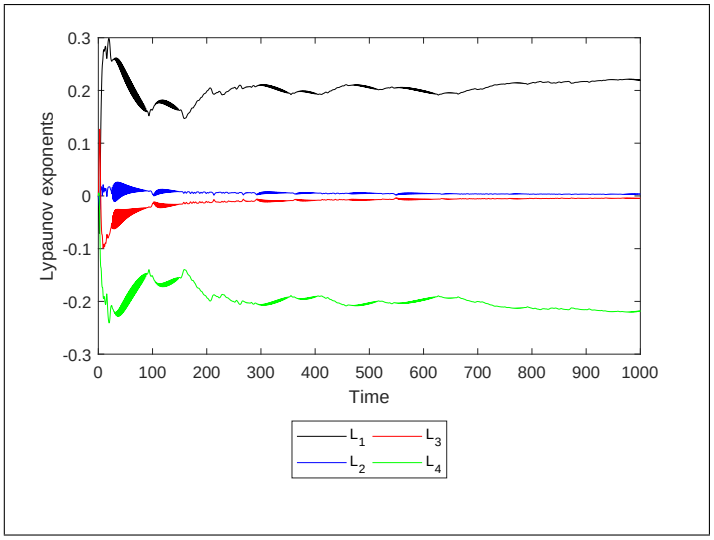

Figure 2.1. Lyapunov exponents for system (2.5).

Since the system is energy conservative the sum of the characteristic exponents is zero. At

least one positive exponent is an indication of chaotic behavior, therefore it can be asserted that this system is chaotic. On the other hand, the phase portraits depicting pure Yang Mills mechanics is shown below.

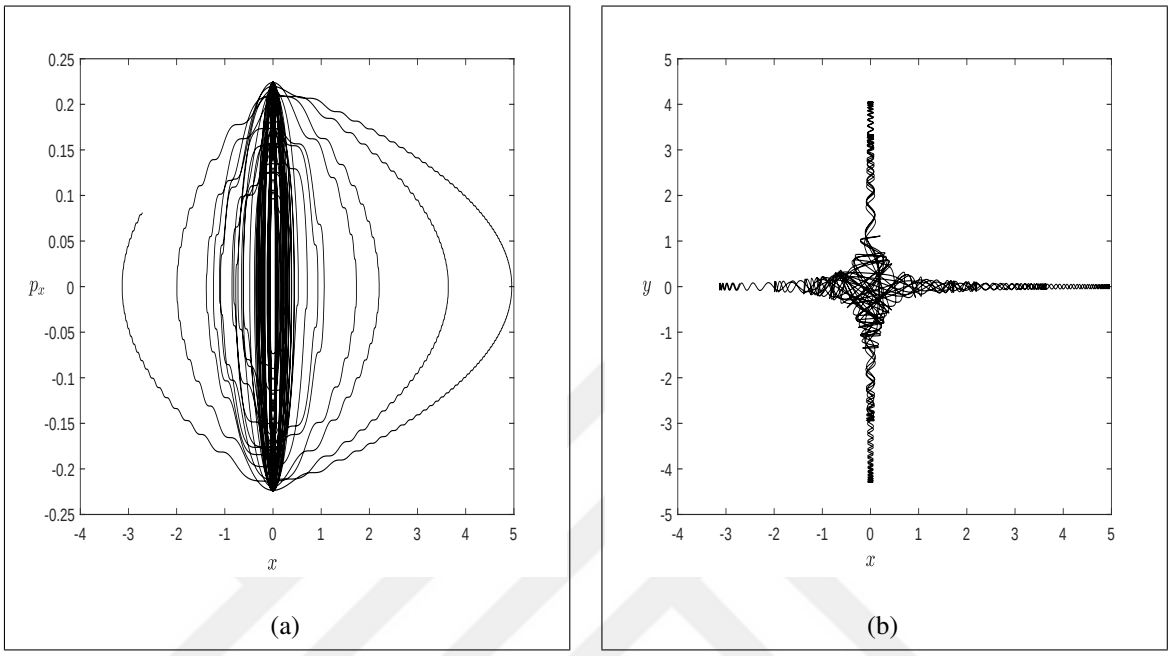

Figure 2.2. Phase portraits showing (a) $x - p_x$. (b) $x - y$

2.2. HIGGS MECHANISM

In gauge theories the realization of different phases is important, since confining phases usually associated with a disordered field configuration and the Higgs phase is associated with globally ordered field configuration. In this part dynamical system involving Higgs field coupled Yang-Mills fields is worked.

The system possesses again gauge group of SU(2) and the corresponding lagrangian is

$$L = -\frac{1}{4}F^a_{\mu\nu}F^{\mu\nu a} + \frac{1}{2}(D_\mu\phi)^*(D^\mu\phi) - V(\phi) \tag{2.7}$$

where D_μ is the covariant derivative defined by

$$(D_\mu\phi) = \partial_\mu\phi - igA^b_\mu T^b\phi \tag{2.8}$$

whith $T^b = \sigma^b/2, b = 1, 2, 3$ are the generators of the SU(2) algebra, and the Higgs potential is the following

$$V(\phi) = \mu^2|\phi|^2 + \lambda|\phi|^4 \tag{2.9}$$

In order to work in dynamical system framework some reductions must be made. We consider a (2+1)-dimensional Minkowski space $\mu = 0, 1, 2$ and homogenous field configuration for both Yang-Mills field and Higgs field[18].

$$\partial_i A^a_\mu = \partial_i \phi = 0, \;\; i = 1, 2 \tag{2.10}$$

Fixing gauge $A^a_0 = 0$ and using reel triplet representation for the Higgs field yields

$$\begin{aligned} L =& \frac{1}{2}(\dot{\vec{A}_1}^2 + \dot{\vec{A}_2}^2) + \dot{\vec{\phi}}^2 - g^2[\frac{1}{2}\vec{A_1}^2\vec{A_2}^2 - \frac{1}{2}(\vec{A_1}\cdot\vec{A_2})^2 + (\vec{A_1}^2 + \vec{A_2}^2)\vec{\phi}^2 \\ & - (\vec{A_1}\cdot\vec{\phi})^2 - (\vec{A_2}\cdot\vec{\phi})^2)] - V(\phi) \end{aligned} \tag{2.11}$$

where $\vec{\phi} = (\phi_1, \phi_2, \phi_3)$, $\vec{A_1} = (A^1_1, A^2_1, A^3_1)$ and $\vec{A_2} = (A^1_2, A^2_2, A^3_2)$.
For $\mu^2 > 0$ V has minimum at $\phi = 0$ but for $\mu^2 < 0$ the minimum is

$$|\vec{\phi_0}| = \sqrt{\frac{-\mu^2}{4\lambda}} = v \tag{2.12}$$

which is the non-zero Higgs vacuum. This vacuum is degenerate and after spontaneous symmetry [19] breaking the physical vacuum can be chosen $\vec{\phi_0} = (0, 0, v)$.With the choice of $A^1_1 = x, A^2_2 = y$ as the non-vanishing components of gauge fields, following Hamiltonian is deduced.

$$H = \frac{1}{2}(\dot{x}^2 + \dot{y}^2) + g^2v^2(x^2 + y^2) + \frac{1}{2}g^2x^2y^2 \tag{2.13}$$

One of the parameters in the above Hamiltonian can be eliminated with the following scale transformation

$$x \to \lambda x, \quad y \to \lambda y, \quad t \to \frac{1}{\lambda} t \tag{2.14}$$

which gives

$$H = \frac{1}{2}(\dot{x}^2 + \dot{y}^2) + \frac{a^2}{2}(x^2 + y^2) + \frac{1}{2}x^2 y^2 \tag{2.15}$$

where $a = \frac{\sqrt{2}v}{\lambda}$. According to physical intuition at high energies associated with strong fields, the quadratic part generated by the Higgs mechanism becomes unimportant and the motion is chaotic. But for weak fields, or sufficiently large values of a in the system(18) the influence of the x^2y^2 gets smaller, so that regular motions become dominant [20, 21].
For numerical investigation Lyapunov exponents are analyzed with the following initial condition for numerical integration $x = 0.1, y = 0.1, \dot{x} = 0.2, \dot{y} = 0.2$. They show a convergence to zero especially for large values of a which is shown below

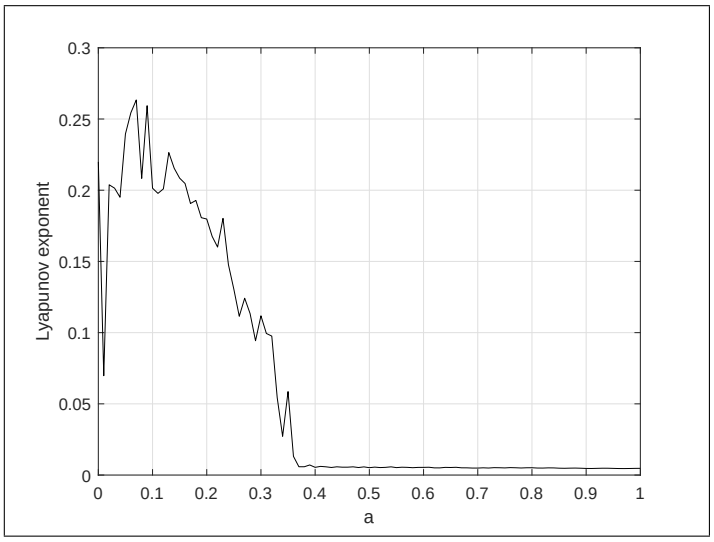

Figure 2.3. Maximal Lyapunov exponents for $0 < a < 1$

On the other hand, for small values of a the system still has positive Lyapunov exponent but there should be a threshold value for a beyond which the system is regular. For this purpose, the variation of maximal lyapunov exponent is analyzed . The parameter a is increased

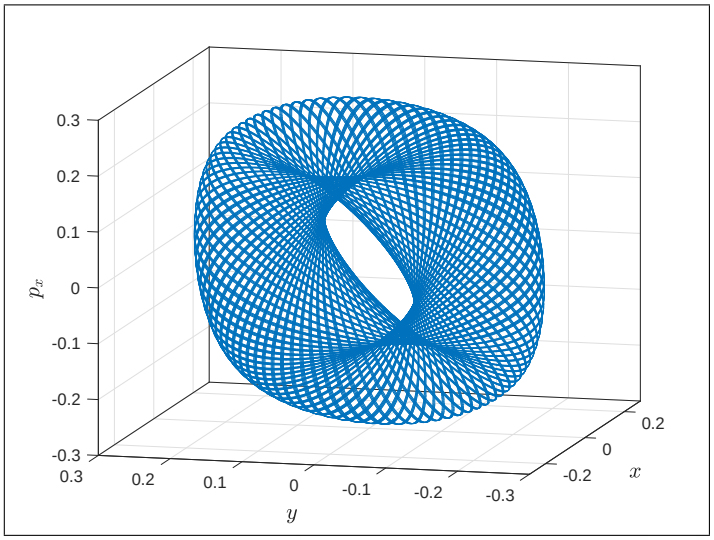

Figure 2.4. Torus for $a = 1$.

from 0 to 1 with a increment of 0.01 and corresponding maximal lyapunov exponents are plotted which is shown in Figure 2.3. In order to avoid possible truncation errors, sufficient integration time is used for each value of a. It is observed that after $a = 0.40$ the largest Lyapunov exponent stays almost constant and is very close to zero. It can be asserted that the non-vanishing Higgs field is responsible for the suppression of chaotic behavior of Yang-Mills fields.

Another important model which exploits Higgs mechanism is the SO(3) Georgi-Glashow model. This model is originally proposed to unify weak and electromagnetic interactions where Higgs mechanism creates massive and massless bosons. However the model is incorrect to describe weak interaction and the correct description is a bit more complicated. The equaition of motions for the model is[20]

$$\begin{aligned}(D_v F^{\mu\nu})^a &= -g\varepsilon^{abc}\phi^b(D_\mu\phi)^c \\ (D_\mu D^\mu\phi)^a &= -\lambda\phi^a(\phi^b\phi^b - \frac{m^2}{\lambda})\end{aligned} \tag{2.16}$$

where $D_\mu^{ab} = \delta^{ab}\partial_\mu + g\varepsilon^{abc}A_\mu^c$ is the covariant derivative. Using the following ansatz

$$A_i^a = \varepsilon_{aij}a_j(t), \quad \phi^a = \sqrt{2}b^a(t) \tag{2.17}$$

using the gauge $A_0^a = 0$ and setting $a^i = x$ and $b^a = y$, yields following simplified equations of motion

$$\begin{aligned} g^{-2}\ddot{x} &= -6y^2x - 3x^3 \\ g^{-2}\ddot{y} &= -6x^2y - 6\lambda g^{-2}y^3 + m^2g^{-2}y \end{aligned} \tag{2.18}$$

These equations can be further simplified, using the suitable scale transformations. Introducing $t \to \alpha t$, $x \to \beta x$, and $y \to \beta y$ where $\alpha = 1/m$ and $\beta = m/g\sqrt{6}$ reduce to following system of equations.

$$\begin{aligned} \ddot{x} &= -xy^2 - \frac{1}{2}x^3 \\ \ddot{y} &= -x^2y - py^3 + y \end{aligned} \tag{2.19}$$

where $p = \lambda/g^2$. The corresponding Hamiltonian is

$$H = \frac{1}{2}(\dot{x}^2 + \dot{y}^2) - \frac{1}{2}y^2 + \frac{1}{2}x^2y^2 + \frac{1}{8}x^4 + \frac{1}{4}py^4 \tag{2.20}$$

For numerical investigation Lyapunov characteristic exponents are analysed with varying p. Numerical results indicating that this system exhibits chaotic motion for wide range of values of parameter p which is shown in Figure 2.5, for small intervals of p system shows hyperchaos[22, 23], with second Lyapunov exponent close to 0.011. It is also remarkable that chaos order transtions take place for some p where largest lyapunov exponents changes dramatically, which is again depicted in Figure 2.5, this behavior is attributed to the Higgs field.

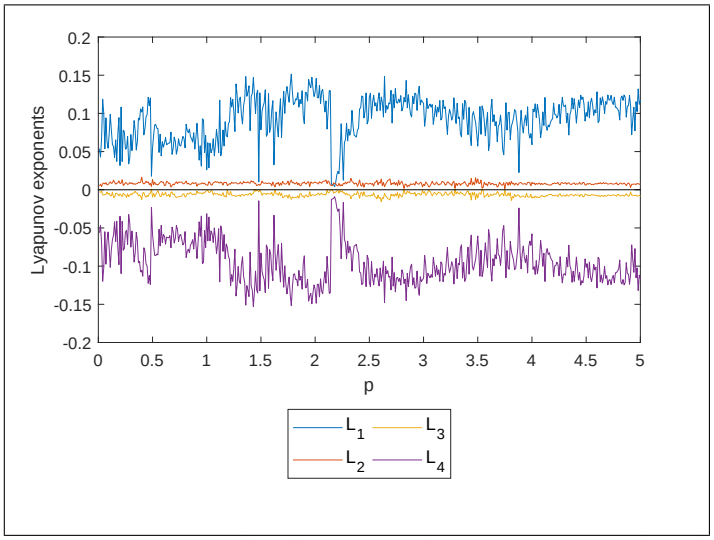

Figure 2.5. Lyapunov exponents for $0 < p < 5$

On the other hand some of the phase portraits indicating chaotic motions in the system are shown below

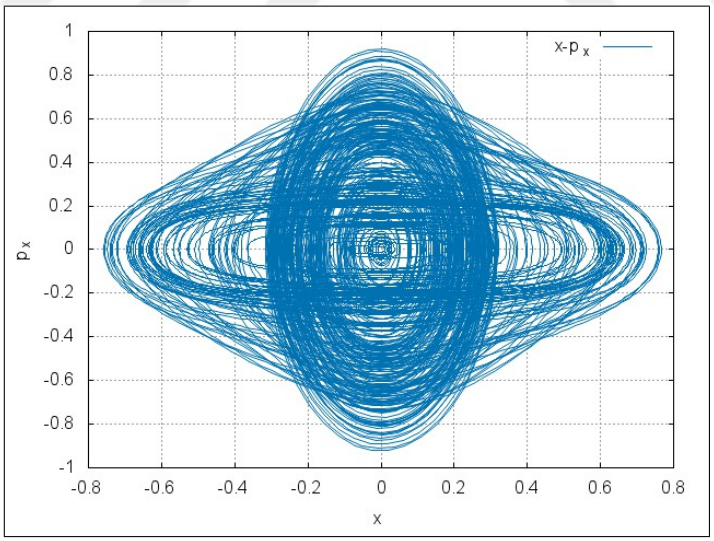

Figure 2.6. Trajectory of $x - p_x$ for $p = 0.2$

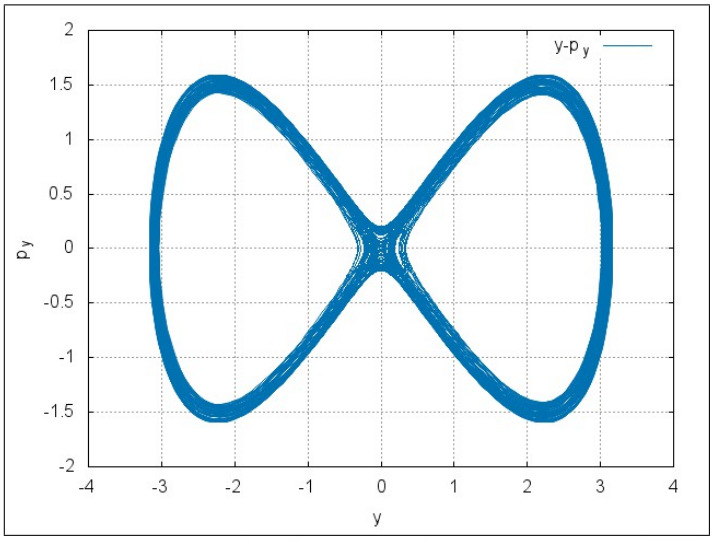

Figure 2.7. Trajectory of $y - p_y$ for $p = 0.2$

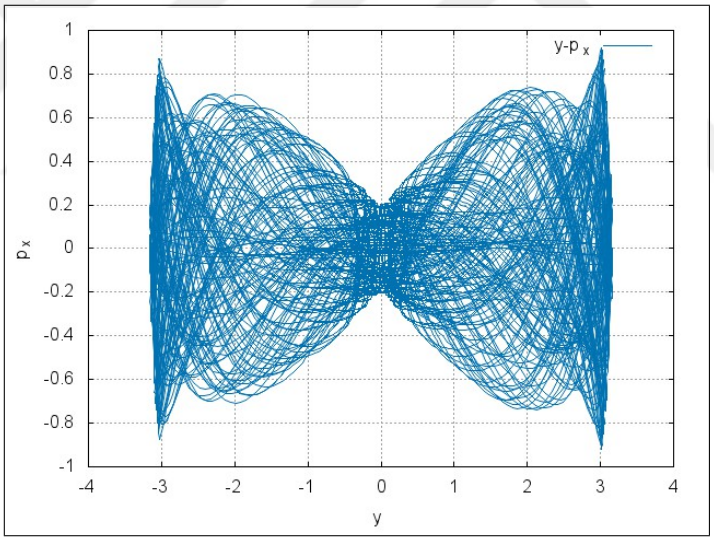

Figure 2.8. Trajectory of $y - p_x$ for $p = 0.2$

2.2.1. Chaos Suppression with Harmonic Oscillator

The system described in eq(2.20) depends strongly on the Higgs parameter p for constant energies. Although for some values of p regular motion is dominant, in general chaotic motion persists for large values of p. From our previous experience in system (2.15) we add

harmonic terms to eq(2.20) . The corresponding Hamiltonian is

$$H = \frac{1}{2}(\dot{x}^2 + \dot{y}^2) + \frac{1}{2}g^2(x^2 + y^2) - \frac{1}{2}y^2 + \frac{1}{2}x^2y^2 + \frac{1}{8}x^4 + \frac{1}{4}py^4 \tag{2.21}$$

To check the chaoticity of the system (2.21) the corresponding equation of motions are integrated with fixed initial conditions of $(0.1, 0.2, 0.1, 0.2)$ and Largest Lyapunov exponents are calculated. Those exponents are then plotted as a surface plot with changing parameters g and p which is shown in Figure 2.9.

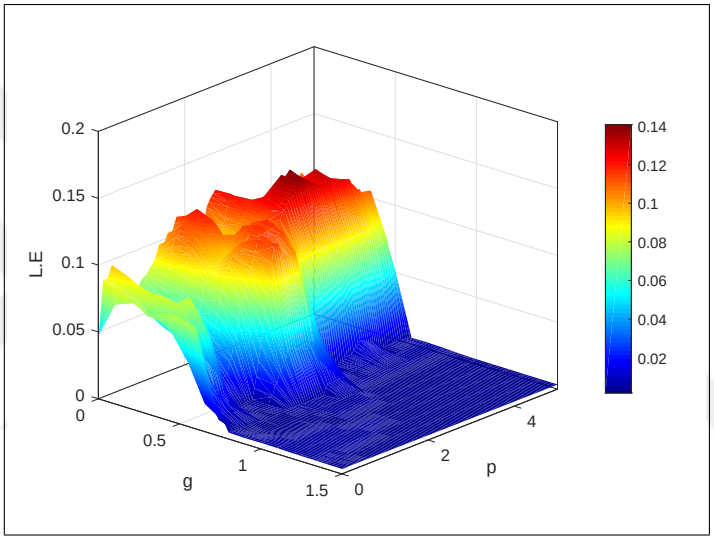

Figure 2.9. Largest Lyapunov exponents

In order to obtain the diagram above, we let parameters change between $0 < p < 5$ and $0 < g < 1.5$. In order to avoid possible truncation errors sufficient integration time is used to obtain Largest Lyapunov exponents. It is remarkable that increasing g suppress the chaotic behaviour since the exponents gets smaller and after $g = 0.75$ they are almost 0. Below there is summary for phase portraits and power spectra plots, which are obtained for changing g.

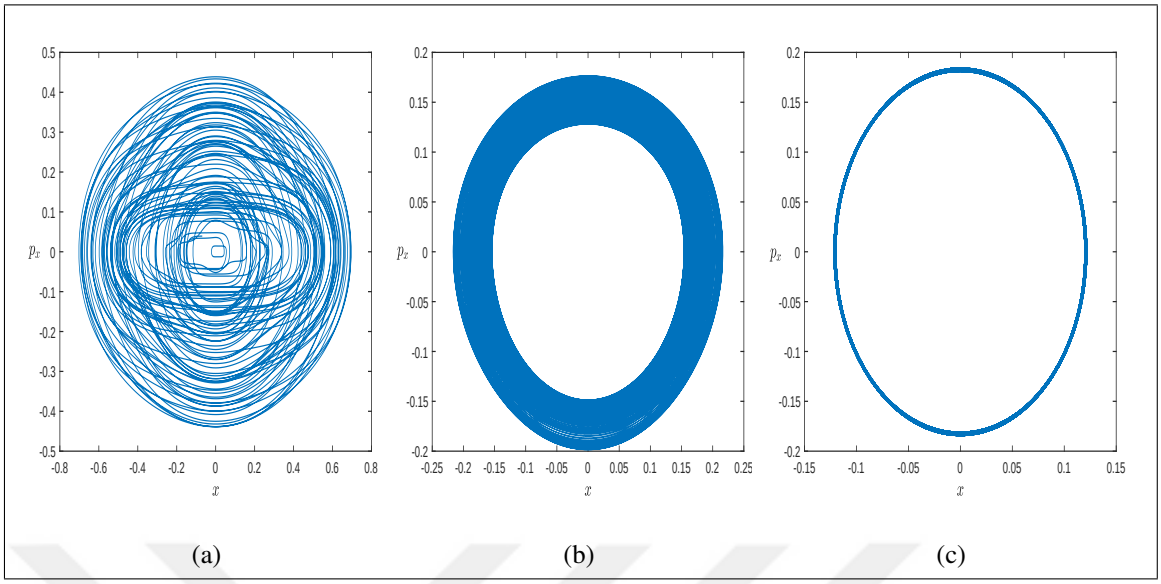

Figure 2.10. Phase portraits of $x - p_x$ for (a) $g = 0$ (b) $g = 0.8$ (c) $g = 1.5$

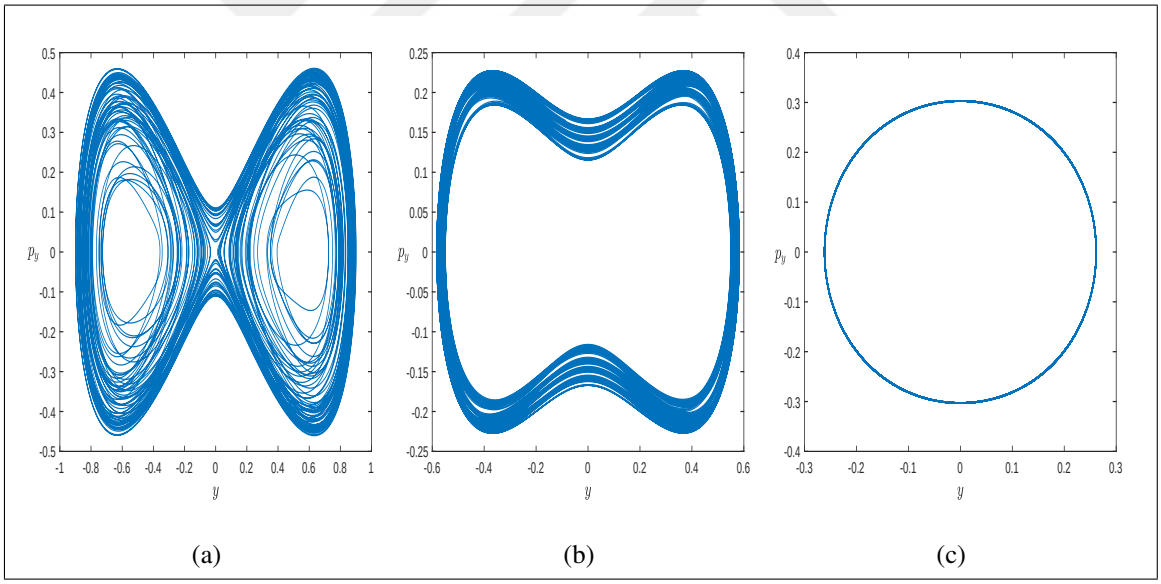

Figure 2.11. Phase portraits of $y - p_y$ for (a) $g = 0$ (b) $g = 0.8$ (c) $g = 1.5$

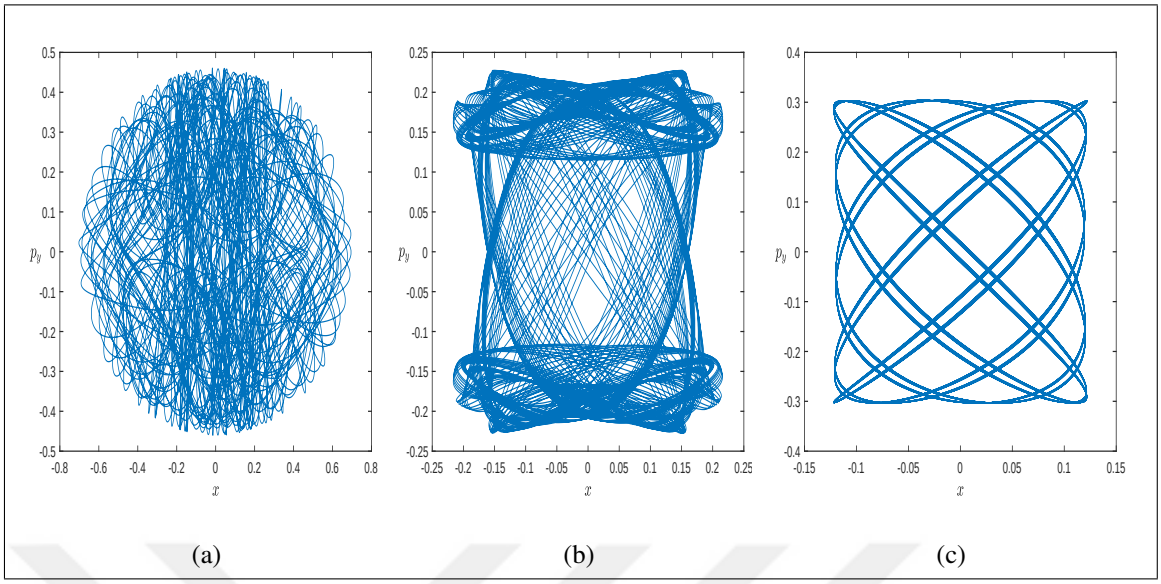

Figure 2.12. Phase portraits of $x - p_y$ for (a) $g = 0$ (b) $g = 0.8$ (c) $g = 1.5$

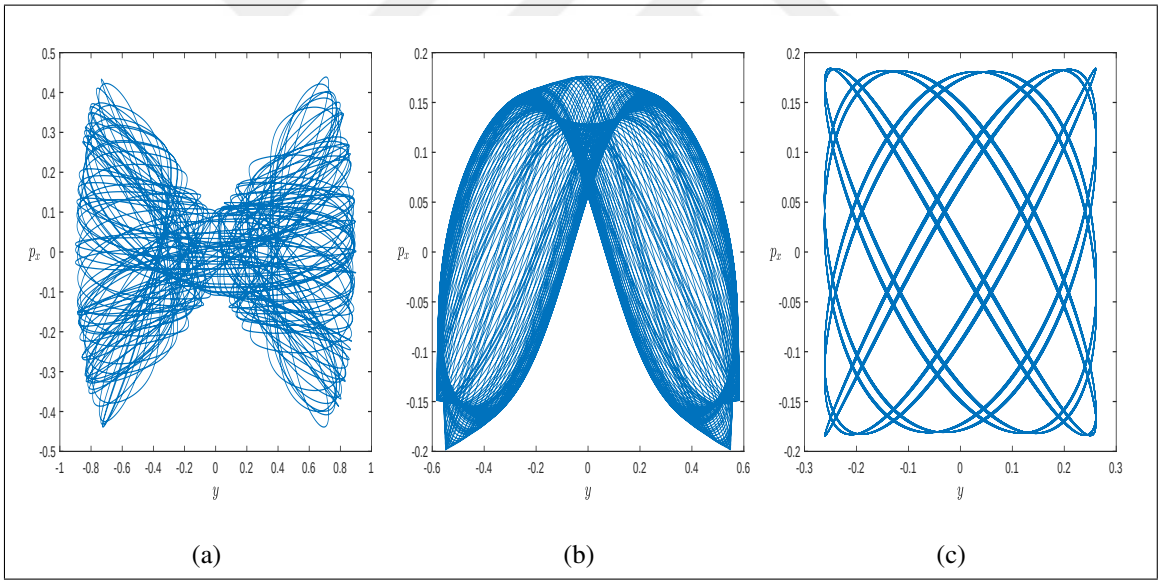

Figure 2.13. Phase portraits of $y - p_x$ for (a) $g = 0$ (b) $g = 0.8$ (c) $g = 1.5$

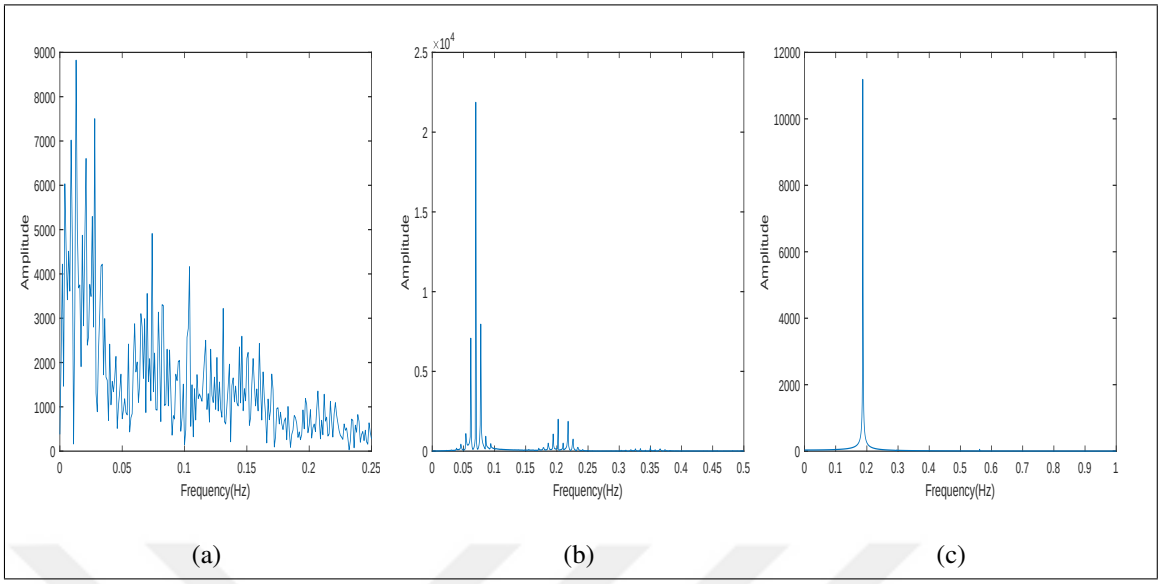

Figure 2.14. Power spectrum for (a) $g = 0$ (b) $g = 0.8$ (c) $g = 1.5$

Beside Lyapunov spectrum, phase portraits and power spectra density plots also give clear indication of stabilizing effect of increasing coefficient of harmonic term in the system. For $g = 0$ chaotic dynamics is dominant which is apparent in power spectra as random peaks are distributed. For $g = 0.8$ quasiperiodic motion becomes dominant in phase portraits, in the power spectrum plot smaller number of peaks observed. Further increasing g up to 1.5 periodic motions take place over the phase portraits and one large peak can be seen in power spectrum.

3. LIE TRANSFORM

Lie Transform[24] is a basic tool for analyzing Hamiltonian Systems in the field of perturbation theory. The technique consists of successive canonical transformation, with manipulation of Lie algebraic methods to bring the Hamiltonian simpler form called normal form. All Hamiltonian perturbation theories are based on performing infinitesimal transformations. The oldest is the Poincaré-Von Zeipel method[25]. The method consists of brute force ordering of the function $F(q, P, t)$ namely the generating function and the Hamilton Jacobi equation. Modified version of this method is constructed by Kolmogorov[26]. By means of successive small transformations rather than a single transformation, Kolmogorov found quadratic expressions. This means that the Hamiltonian can be transformed successively to orders of $\varepsilon, \varepsilon^2, \varepsilon^4, \varepsilon^8$...

Great improvement in Hamiltonian perturbation theory was brought with the introduction of Lie Transforms by Hori[27]. Lie Transform technique is simpler since no functions of mixed variables needed, and all the terms are generated with Poisson brackets, making this theory canonically invariant. Deprit[28] improved the method to obtain expressions for n^{th} order term of an expansion of the transformation in a power series of in ε. Lie Transform method has been used to study magnetic moment invariance in a dipole field by Dragt and Finn[29, 30]. The technique is based on infinite product of Lie transformations and is particularly effective for higher order calculations.

3.1. METHOD OF DRAGT AND FINN

In this section we briefly introduce the methodology to normalize a given Hamiltonian over an example which is structurally similar to the cases that we used in section 2.
Considering a class of systems given by the Hamiltonian

$$H(\mathbf{p},\mathbf{q}) = \frac{1}{2}({p_x}^2 + {p_y}^2) + V(x,y) \tag{3.1}$$

where V is the potential of the system possessing an absolute minimum and reflection symmetries in both coordinates

$$x \longrightarrow -x, \qquad y \longrightarrow -y,$$

which is also present in the whole Hamiltonian. The potential can be expanded as

$$V(x,y) = \sum_{n=0}^{\infty} \varepsilon^n V_n(x,y) \tag{3.2}$$

and the Hamiltonian can be transformed to

$$K(\mathbf{P},\mathbf{Q}) = \sum_{n=0}^{\infty} \varepsilon^n K_n(\mathbf{P},\mathbf{Q}) = M_g^{-1} H(\mathbf{p},\mathbf{q}) \tag{3.3}$$

where $\mathbf{P}, \mathbf{Q}$ are the new coordinates resulting from a Canonical Transformation

$$(\mathbf{P},\mathbf{Q}) = M_g(\mathbf{p},\mathbf{q}) \tag{3.4}$$

The linear differential operator M_g is defined by a succession of Lie transformation

$$M_g = e^{-\varepsilon L_{g_1}} e^{-\varepsilon^2 L_{g_2}} \cdots e^{-\varepsilon^n L_{g_n}} \cdots \tag{3.5}$$

where g_n's are the generating functions of the corresponding canonical transformation, and the linear differential operator L_S is the Lie Derivative defined by the following way.

Given two real and analytic functions f and S in Ω, bounded domain of the $2n$-dimensional manifold $\{(\mathbf{p},\mathbf{q})\} = \mathbb{M}^{2n}$, the Lie Derivative of the function f with respect to S, the Poisson bracket (S,f), which is also denoted by the symbol

$$L_S f = (S,f) = \sum_{l=1}^{n} \left(\frac{\partial S}{\partial q_l}\frac{\partial f}{\partial p_l} - \frac{\partial S}{\partial p_l}\frac{\partial f}{\partial q_l} \right) \tag{3.6}$$

The Lie series associated to S or to (L_S) applied to f is defined by

$$e^{\varepsilon L_S} f = \sum_{k=0}^{\infty} \frac{\varepsilon^k}{k!} L_S^k f \tag{3.7}$$

where $L_S^k f$ is defined inductively by

$$L_S^0 f = f\,, \qquad L_S^n f = L_S\left(L_S^{n-1} f\right) \tag{3.8}$$

The transformation introduced by Dragt and Finn given in equation (6) can be written as

$$M_g = I + \sum_{n=1}^{\infty} \varepsilon^n M_n \tag{3.9}$$

By inspection of equation (6) the terms in the series become

$$M_n = \sum_{m_1+2m_2+\cdots+nm_n=n} (-1)^{m_1+m_2+\cdots+m_n} \frac{L_{g_1}^{m_1} L_{g_2}^{m_2} \cdots L_{g_n}^{m_n}}{m_1! m_2! \cdots m_n!} \tag{3.10}$$

On the other hand, the inverse transformation given by

$$M_g^{-1} = e^{\varepsilon L_{g1}} e^{\varepsilon^2 L_{g2}} \cdots e^{\varepsilon^n L_{gn}} \cdots \tag{3.11}$$

can also be written as

$$M_g = I + \sum_{n=1}^{\infty} \varepsilon^n M_n^{-1} \tag{3.12}$$

The coefficients in the inverse transformation becomes

$$M_n^{-1} = \sum_{m_1+2m_2+\cdots+nm_n=n} \frac{L_{g_n}^{m_n} L_{g_{n-1}}^{m_{n-1}} \cdots L_{g_1}^{m_1}}{m_n! m_{n-1}! \cdots m_1!} \tag{3.13}$$

By expanding in power series the new Hamiltonian in equation (3) and equating the coefficients of the same order one obtains a set of equations

$$\begin{aligned} K_0 =& H_0 \\ & \cdots \\ K_n =& L_{g_n} H_0 + R_n \\ & \cdots \\ & \cdots \end{aligned} \tag{3.14}$$

where

$$R_n = H_n + \sum_{m_1+2m_2+\cdots+(n-1)m_{n-1}=n} \frac{L_{g_{n-1}}^{m_{n-1}} \cdots L_{g_2}^{m_2} L_{g_1}^{m_1}}{m_{n-1}! \cdots m_2! m_1!} + \sum_{k=1}^{n-1} M_k H_{n-k} \tag{3.15}$$

The n^{th} equation of (14) the so called homological equation which can be written as

$$L_{H_0} g_n + K_n = R_n \tag{3.16}$$

The rest of R_n contains terms which are known if the preceding $n-1$ equations have been solved.

The new Hamiltonian is in "normal form" up to degree n if

$$\{H_0, K_r\} = 0 \tag{3.17}$$

satisfied $\forall r \leqslant n$. This means that the homological equation(14) must be solved with the condition (17) at any order.

3.2. APPLICATION TO SPECIFIC PROBLEMS

In this part the methodology described above is applied to our system (2.15) and system (2.21). But for the sake of simplicity we describe the procedure over system(2.15) step by step and not for (2.21) since similar algebra is involved. On the other hand the results obtained from the analysis and numerical results are presented for both case.
First system that we use to study normalization scheme is system (2.15).

$$H = \frac{1}{2}\left(p_x^2 + p_y^2\right) + \frac{a^2}{2}\left(x^2 + y^2\right) + \frac{1}{2}\,x^2y^2 \tag{3.18}$$

which describes the central part of elliptical galaxies without escape.
The system can be considered as the Hamiltonian of two coupled harmonic oscillators and a quartic nonlinearity as a perturbation term[31], where a describes the mass of gauge fields acquired by Higgs mechanism. The coefficient of perturbation term is relatively small so that the system is amenable to analysis with perturbation theory. Structurally similar Hamiltonian was studied by Contopoulos[32], that is also known as Contopoulos Hamiltonian which describes the central part of elliptical galaxies without escape.
Hamiltonian(3.18) can be expanded as a series

$$H\left(x, y, p_x, p_y\right) = \sum_{n=0}^{\infty} \varepsilon^n H_n\left(x, y, p_x, p_y\right) \tag{3.19}$$

The components H_n are the following

$$H_0 = \frac{1}{2}\left(p_x^2 + w_1^2 x^2\right) + \frac{1}{2}\left(p_y^2 + w_2^2 y^2\right) \tag{3.20}$$

$$H_2 = \frac{1}{2}x^2y^2 \tag{3.21}$$

$$H_n = 0 \qquad \forall n \neq 0, 2 \tag{3.22}$$

where $w_1 = w_2 = v$.

With the aid of following scale transformations

$$x = \frac{q_1}{\sqrt{w_1}}, \qquad y = \frac{q_2}{\sqrt{w_2}}$$

$$p_x = p_1\sqrt{w_1}, \qquad p_y = p_2\sqrt{w_2}$$

Hamiltonian (3.18) can be put in more convenient form

$$H\left(\mathbf{p}, \mathbf{q}\right) = \frac{1}{2}\sum_{l=1}^{2} w_l \left(p_l^2 + q_l^2\right) + \frac{1}{2w_1w_2}q_1^2q_2^2 \tag{3.23}$$

With a symplectic change of variables given by

$$\begin{aligned} x_l &= \frac{1}{\sqrt{2}}\left(q_l + ip_l\right) \\ y_l &= \frac{i}{\sqrt{2}}\left(q_l - ip_l\right) \end{aligned} \tag{3.24}$$

H_0 becomes

$$H_0 = -i\sum_{l=1}^{2} w_l x_l y_l \tag{3.25}$$

and the Lie operator becomes

$$L_{H_0} = i\sum_{l=1}^{2} w_l \left(x_l\frac{\partial}{\partial x_l} - y_l\frac{\partial}{\partial y_l}\right) \tag{3.26}$$

for $l = 1, 2$ The action of L_{H_0} on any monomial is given by

$$L_{H_0}(x_1^{\lambda_1} x_2^{\lambda_2} y_1^{\kappa_1} y_2^{\kappa_2}) = \sum_{l=1}^{2} (w_l \lambda_l - w_l \kappa_l)\, x_1^{\lambda_1} x_2^{\lambda_2} y_1^{\kappa_1} y_2^{\kappa_2} \tag{3.27}$$

Monomials that appear in the normal form must be in the Kernel of L_{H_0}, this implies right hand side of equation (3.27) is equal to zero, or using inner product notation

$$\boldsymbol{\omega}.(\boldsymbol{\lambda} - \boldsymbol{\kappa}) = 0 \tag{3.28}$$

The rest of the calculations are done considering $w_1 = w_2 = 1$ with the values of parameters $g = 1$ and $a = \frac{1}{\sqrt{2}}$.
Regarding 1-1 resonance relation of frequencies $\boldsymbol{\omega} = (1, 1)$ equation(3.28) becomes

$$\lambda_1 + \lambda_2 = \kappa_1 + \kappa_2 \tag{3.29}$$

Any monomials satisfying condition (3.29) are called resonant monomials and they appear in the normalized Hamiltonian. The other monomials can be eliminated with the proper choice of generating function .
For $n = 0$ we have

$$K_0 = H_0 \tag{3.30}$$

For $n = 1$ we must have $K_1 = 0, \quad g_1 = 0$ due to symmetric structure of the problem[33].
For the case $n = 2$ we must solve

$$K_2 + L_{H_0} g_2 = H_2 \tag{3.31}$$

In the new variables the second order terms in the Hamiltonian becomes

$$H_2 = \frac{1}{8}(x_1^2x_2^2 - 2ix_1^2x_2y_2 - x_2^2y_1^2 - 2ix_1^2x_2y_2 - 4x_1x_2y_1y_2 + 2ix_2y_1^2y_2 - x_1^2y_2^2 + 2ix_1y_1y_2^2 + y_1^2y_2^2) \tag{3.32}$$

The only monomials that cannot be eliminated in K_2 are

$$K_2 = -\frac{1}{8}(4x_1x_2y_1y_2 + x_1^2y_2^2 + x_2^2y_1^2) \tag{3.33}$$

The details of the procedure for the normalization can be found in [9, 34].
By applying the procedure above to the Hamiltonian, we have found the normal forms up to order 6. The normalized Hamiltonian has the form

$$K = K_0 + \varepsilon^2K_2 + \varepsilon^4K_4 + \varepsilon^6K_6 + O(\varepsilon^8) \tag{3.34}$$

One advantage of this algorithm is that one can construct approximate integral beside the normalization process. In the new Hamiltonian H_0 is an integral of motion due to equation (3.17). So, one can choose the function

$$I = K - H_0 \tag{3.35}$$

as a second integral of motion conveying approximate information of the dynamics in original system. Denoting it as power series

$$I = \sum_{n=0}^{\infty} \varepsilon^n I_n \tag{3.36}$$

The terms of the integral are given by[9]

$$I_n = H_n - K_n + \sum_{m=1}^{n-1} M_{n-m}[H_m - I_m], \qquad n \geqslant 1. \tag{3.37}$$

The integral of motion has the same structure of the normalized Hamiltonian.

$$I = I_0 + \varepsilon^2 I_2 + \varepsilon^4 I_4 + \varepsilon^6 I_6 + O(\varepsilon^8) \tag{3.38}$$

We do not present here the explicit forms of expressions for the normalized Hamiltonian and approximate integrals since they are algebraically cumbersome and they take so much place, but the reader can find the approximated expressions up to order 6 in the appendix.

3.3. TIME DEPENDENCE OF APPROXIMATE INTEGRALS

An important issue for those integrals obtained above is their asymptotic behaviour. The algorithm to obtain approximate integrals does not give any information about the convergence of the obtained series. Indeed, for higher order of truncations the series turn out to be divergent. Although it is analytically difficult to obtain a result for which order of truncation is most suited, instead time variation of truncated series is analyzed numerically. Some of them particularly have smaller fluctuations then the other ones.

3.3.1. Integrals for System (2.15)

Before performing numerical analysis, it is more convenient to use action angle coordinates. Using canonical equation of motions new equation of motions are obtained and then integrated numerically with suitable initial conditions. In terms of action angle coordinates given by

$$\begin{aligned} q_1 &= \sqrt{\frac{2J_1}{w_1}}\cos\theta_1, \qquad p_1 = -\sqrt{2J_1 w_1}\sin\theta_1 \\ q_2 &= \sqrt{\frac{2J_2}{w_2}}\cos\theta_2, \qquad p_1 = -\sqrt{2J_2 w_2}\sin\theta_2 \end{aligned} \tag{3.39}$$

Hamiltonian (2.15) can be written in terms of action angle coordinates as

$$H = J_1 + J_2 + 4\alpha J_1 J_2 \cos^2\theta_1 \cos^2\theta_2 \tag{3.40}$$

where the frequencies are $w_1 = w_2 = 1$, and α corresponds to the parameter of the quartic term in the original system which is $\alpha = \frac{1}{2}$ for our specified values of parameters.
Using the canonical equation of motions

$$\dot{J}_i = -\frac{\partial H}{\partial \theta_i}, \qquad \dot{\theta}_i = \frac{\partial H}{\partial J_i} \tag{3.41}$$

following equation of motions are derived.

$$\begin{aligned}
\dot{J}_1 &= 8\alpha J_1 J_2 \cos\theta_1 \sin\theta_1 \cos^2\theta_2 \\
\dot{J}_2 &= 8\alpha J_1 J_2 \cos\theta_2 \sin\theta_2 \cos^2\theta_1 \\
\dot{\theta}_1 &= 4\alpha J_2 \cos^2\theta_1 \cos^2\theta_2 + 1 \\
\dot{\theta}_2 &= 4\alpha J_1 \cos^2\theta_1 \cos^2\theta_2 + 1
\end{aligned} \tag{3.42}$$

Above equations are integrated numerically for initial conditions of $J_1(0) = 1.0$, $J_2(0) = 1.0$, $\theta_1(0) = 0.0$, $\theta_2(0) = 0.5$. Some of the important results are shown below.

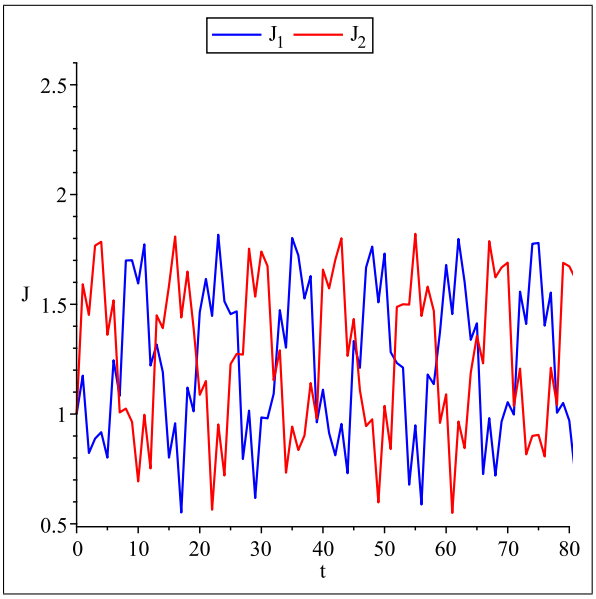

Figure 3.1. Oscillation of $J_1$and J_2 vs time

Time dependence of $J_1$and J_2 is shown in Figure 3.5. Resonance relation between unperturbed frequencies generates energy transfer between the two modes, the period of their oscillation is nearly $T \approx 12$ which is close to $\left(\frac{2\pi}{\alpha}\right)$. This can be also seen from the graph in Figure 3.2, where the slow parts of the relative phases are plotted for a time span of 60.

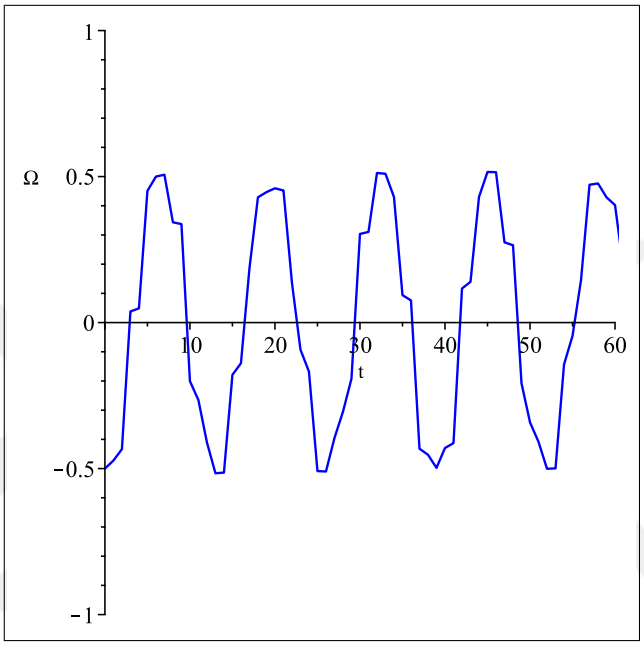

Figure 3.2. Time dependence of relative phase $\Omega = \theta_1 - \theta_2$

From Figure 3.5 one can conclude that $J_1$and J_2 can not be considered as constants of motion separately. But the their sums can be regarded approximately constant[35].

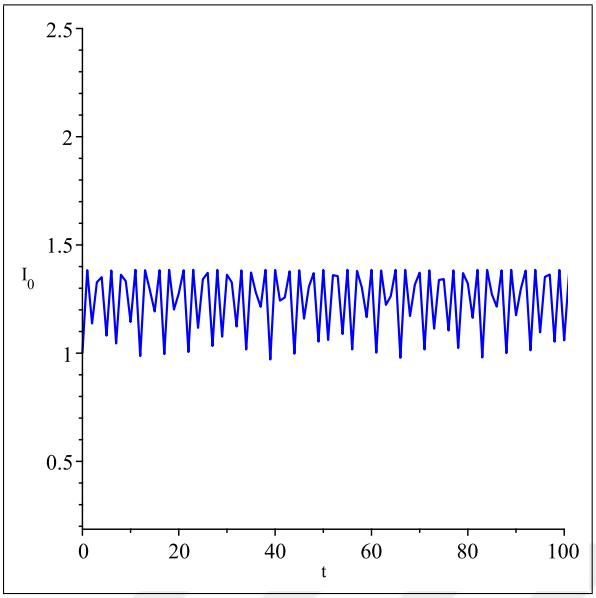

Figure 3.3. Time dependence of I_0

In Figure 3.3 the oscillatory change in $I_0 = J_1 + J_2$ is depicted. The amplitude of the oscillation gets small. For Higher orders the formal integrals are also plotted. In general there is an optimal truncation order, beyond this order the integrals are getting diverge[36]. Figure 3.4 depicts the evolution of I_2 and I_4. For the problem under consideration 4^{th} order truncation seems the best candidate in which the amplitude of the oscillation is very small and it can be considered as a formal constant of motion.

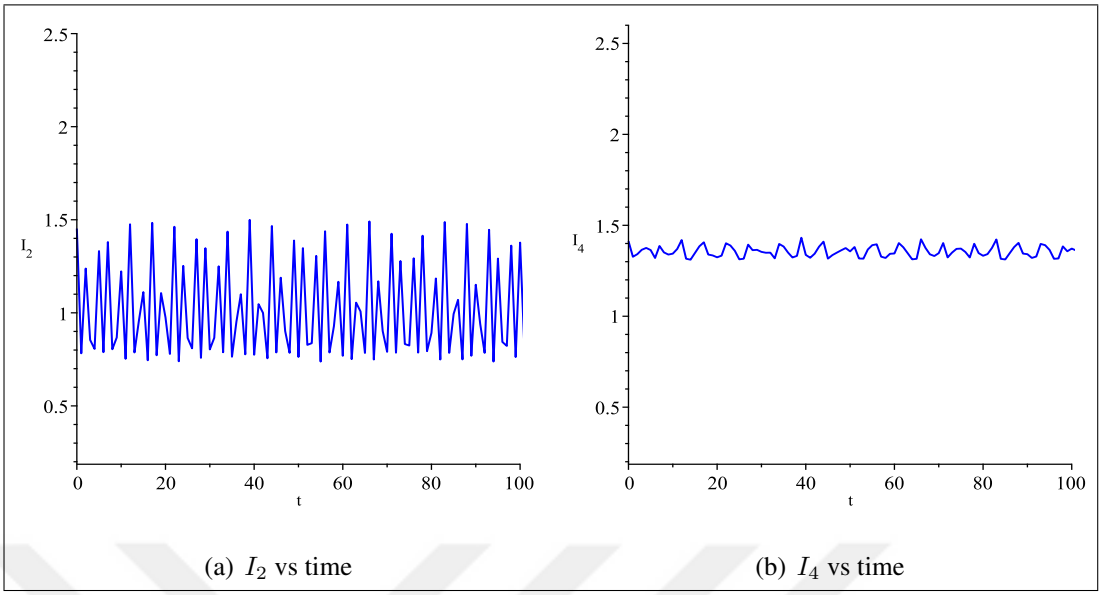

(a) I_2 vs time (b) I_4 vs time

Figure 3.4. Time dependence of (a) I_2 (b) I_4

3.3.2. Integrals for System (2.21)

The Same procedure is used to observe the fluctuations in the truncated integrals of the system 2.21. The corresponding Hamiltonian is given by in terms of action angle coordinates as

$$H = J_1 + J_2 + \frac{1}{2}J_1^2\cos^4\theta_1 + \frac{1}{2}J_2^2\cos^4\theta_2 + 4\alpha J_1 J_2\cos^2\theta_1\cos^2\theta_2 \tag{3.43}$$

Similar to system 2.15 the frequencies are chosen to be $w_1 = w_2 = 1$, and the quartic coupling coefficient is $\alpha = \frac{1}{2}$. Above Hamiltonian yields the following equations of motion

$$\begin{aligned}
\dot{J}_1 &= 8\alpha J_1 J_2\cos\theta_1\cos^2\theta_2\sin\theta_1 + 2J_1^2\cos^3\theta_1\sin\theta_1 \\
\dot{J}_2 &= 8\alpha J_1 J_2\cos^2\theta_1\cos\theta_2\sin\theta_2 + 2J_2^2\cos^3\theta_2\sin\theta_2 \\
\dot{\theta_1} &= 4\alpha J_2\cos^2\theta_1\cos^2\theta_2 + J_1\cos^4\theta_1 + 1 \\
\dot{\theta_2} &= 4\alpha J_1\cos^2\theta_1\cos^2\theta_2 + J_2\cos^4\theta_2 + 1
\end{aligned} \tag{3.44}$$

Above equations are integrated numerically for initial conditions of $J_1(0) = 0.5$, $J_2(0) = 0.5$, $\theta_1(0) = 1.0$, $\theta_2(0) = 0.0$. Time dependence of truncated integrals are plotted, results are shown below

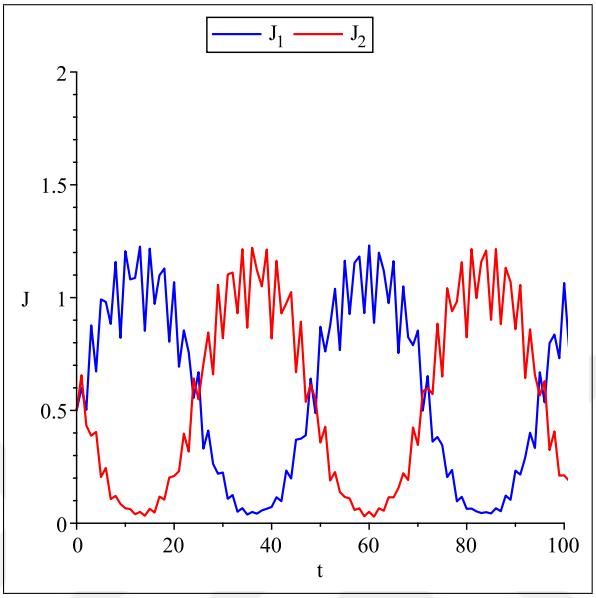

Figure 3.5. Oscillation of $J_1$and J_2

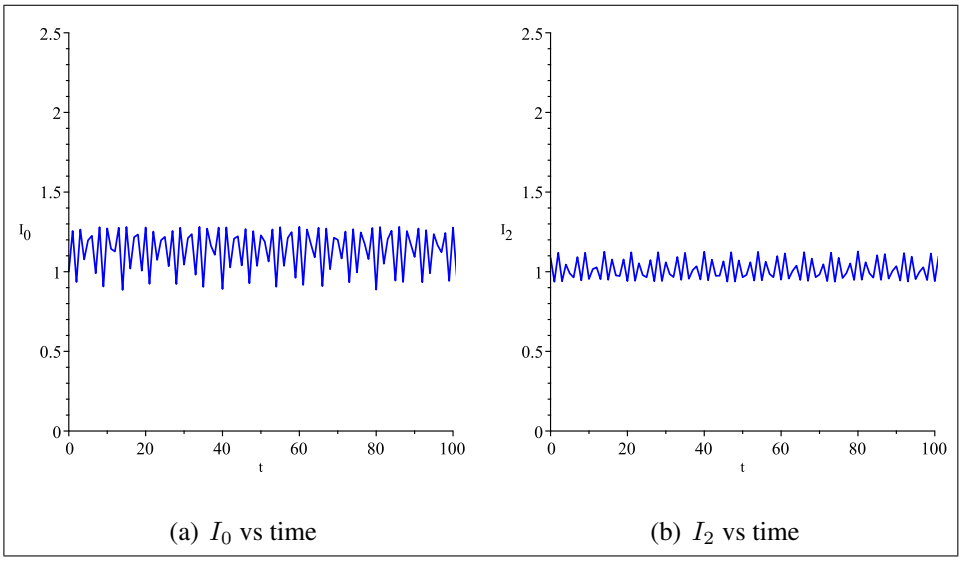

(a) I_0 vs time (b) I_2 vs time

Figure 3.6. Time dependence of (a) I_0 (b) I_2

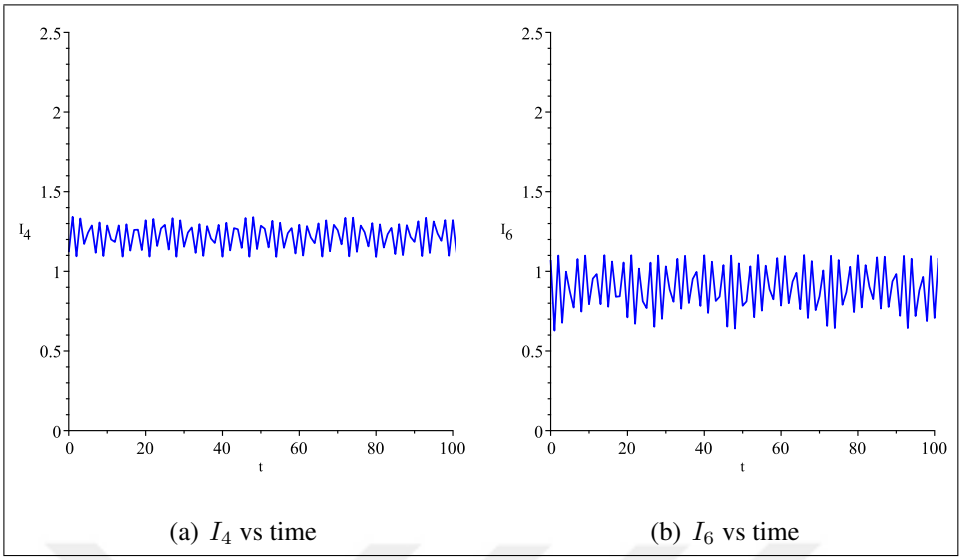

(a) I_4 vs time (b) I_6 vs time

Figure 3.7. Time dependence of (a) I_4 (b) I_6

3.4. COMPUTATION OF PERIODIC ORBITS

Normal forms of Hamiltonian system[37, 38] described above are used to compute periodic orbits. Using "action-angle" like variables J, θ defined by the following coordinate transformations

$$Q_1 = \sqrt{2J_1}\cos\theta_1, \qquad Q_2 = \sqrt{2J_2}\cos\theta_2, \tag{3.45}$$

$$P_1 = \sqrt{2J_1}\sin\theta_1, \qquad P_2 = \sqrt{2J_2}\sin\theta_2, \tag{3.46}$$

Typical structure of a doubly symmetric Resonance normal form truncated at minimum order is[32, 39]

$$K = m_1 J_1 + m_2 J_2 + \sum_{k=2}^{m_1+m_2} P^{(k)}(J_1, J_2) + \\ a_{m_1 m_2} J_1^{m_2} J_2^{m_1} \cos\left[(2m_2\theta_1 - 2m_1\theta_2)\right] \tag{3.47}$$

where $P^{(k)}$ are homogenous polynomials of order k and $a_{m_1 m_2}$ are coefficients of the resonant terms. For a non-resonant(Birkhoff) normal form the coefficients $a_{m_1 m_2}$ vanish so that the normalized Hamiltonian becomes independent from angles. Therefore, J becomes true conserved action and the solutions become

$$Q_1(t) = \sqrt{2J_1}\cos\theta_1, \quad Q_2(t) = \sqrt{2J_2}\cos(\theta_2 + \theta_0) \tag{3.48}$$

and the frequencies can be found by $\dot{\theta} = \frac{\partial K}{\partial J}$

However, in the resonant case, it is not possible to write the solutions in closed form in terms of elementary functions, but solutions can still be worked in the case of main periodic orbits for which J, θ are again true action angle variables.

Analytical expressions are found corresponding to each family of periodic orbits with the inverse transformations for the coordinates. The expressions are in the form of truncated power series and they can be compared with the numerical solutions with suitable initial conditions.

Using the generating function the solutions in terms of original coordinates can be obtained using the inverse transformation(13). The transformation back to original variables can be expressed as a series

$$x(t) = x_1 + x_2 + x_3 + \cdots \tag{3.49}$$

where

$$
\begin{aligned}
x_1 &= Q \\
x_2 &= 0 \\
x_3 &= L_2(Q) = \{g_2, Q\} \\
x_4 &= 0 \\
x_5 &= L_4(Q) + \frac{1}{2}L_2^2(Q) = \{g_4, Q\} + \frac{1}{2}\{g_2, \{g_2, Q\}\} \\
&\vdots
\end{aligned}
\tag{3.50}
$$

For a general system of (41) periodic orbits can be specified as follows[40]

1 - Periodic orbits corresponding to normal modes solutions namely $J_1 = 0$, or $J_2 = 0$

2 - Periodic orbits in general position that corresponds to fixed phase difference between the two angles, $m_2\theta_1 - m_1\theta_2 = \theta_0$

In both cases the solutions retain a form similar to (42).

3.4.1. Periodic Solutions for System (2.15)

For the normal mode solutions, the orbit along the symmetry axes are simple periodic orbits, they also known as axial orbits[40]. Requiring $J_1 = 0$ or $J_2 = 0$ the normalized Hamiltonian becomes $K = J_2$ and $K = J_1$ respectively. They represent simple harmonic motion with

frequency equal to 1, the solutions are

$$q_2 = A\sin(\theta+\phi), \quad q_1 = 0 \tag{3.51}$$

$$q_1 = A\sin(\theta+\phi), \quad q_2 = 0 \tag{3.52}$$

where $A = q(0)$ and ϕ is phase difference.

Another family of periodic orbit correspond to $q_1 = \pm q_2$. This is a special case for $m_2\theta_1 - m_1\theta_2 = \theta_0 = 0$, their solutions represent inclined family of periodic orbits

The expression for K is given up to perturbation order 6 by

$$K = 2J_1 + \frac{3}{4}J_1^2 - \frac{17}{32}J_1^3 + \frac{375}{512}J_1^4 \tag{3.53}$$

It should be noted that one degree of freedom is removed from the system, and K becomes independent of one of the J's. The absence of angular terms gives the possibility to write the solutions in power series. In terms of nomalized variables the solution will have the form of $Q_1 = Q_2 = A\cos\theta$. The expressions obtained for the coordinates and the frequency are the following

$$\begin{aligned} q_1 = {} & A\cos\theta - \frac{3}{16}A^3\cos\theta + \frac{1}{32}A^3\cos 3\theta + \frac{303}{2048}A^5\cos\theta - \frac{39}{1024}A^5\cos 3\theta \\ & + \frac{1}{1024}A^5\cos 5\theta - \frac{1263}{8192}A^7\cos\theta + \frac{3219}{65536}A^7\cos 3\theta - \frac{73}{32768}A^7\cos 5\theta \\ & + \frac{1}{32768}A^7\cos 7\theta \end{aligned}$$

$$q_2 = \pm\, q_1$$

$$\dot{\theta} = 2 + \frac{3}{4}A^2 - \frac{51}{128}A^4 + \frac{375}{1024}A^6 \tag{3.54}$$

For the quality of the obtained results, comparisons made with the numerical solution. The resulting systems of differential equations from the original Hamiltonian is integrated numerically, with initial conditions of $q_1 = 0.48$ and $p_1 = 0.50$, which correspond to $E \approx 0.50$. For the analytic expressions (48) the amplitude A is obtained choosing $\theta = 0$ at $t = 0$.

Phase space variables are plotted along the numerical solutions which is depicted in Figure 3.8. On the other hand, time dependence of q_1 is plotted along the numerical solution up to timescale of 20 which is shown in Figure 3.9. There exists a small difference in terms of amplitude of the motion for corresponding solutions, which becomes even smaller for lower values of energy. Apart from this good agreement is achieved for the shape and the frequency of the solutions.

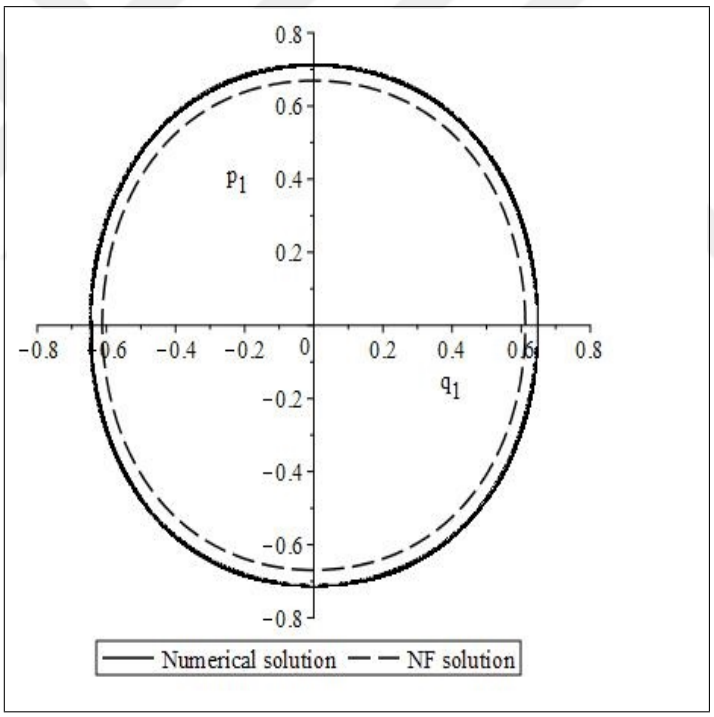

Figure 3.8. Comparison of numerical and normal form solution for $E \approx 0.50$

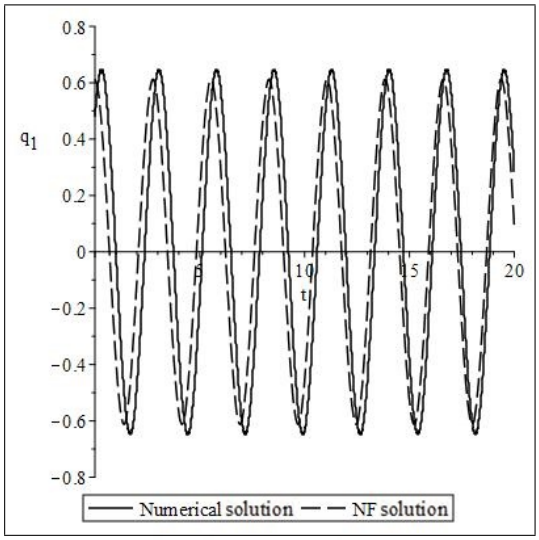

Figure 3.9. Comparison of numerical and normal form solution for $E \approx 0.50$

Another family of periodic orbit is the loop orbit. These orbits correspond to $m_2\theta_1 - m_1\theta_2 = \theta_0 = \pm\pi/2$ and they represent in-phase oscillation and antiphase oscillation respectively. The normalized Hamiltonian takes the form

$$\begin{aligned} K =& J_1 + J_2 + \frac{1}{4}J_1J_2 - \frac{1}{64}J_1J_2^2 - \frac{1}{64}J_1^2J_2 + \frac{11}{1024}J_1J_2^3 \\ &+ \frac{11}{1024}J_1^3J_2 - \frac{7}{256}J_1^2J_2^2 \end{aligned} \tag{3.55}$$

In terms of normalized variables, the form of solution can be written as $Q_1 = A\cos\theta$, $Q_2 = A\sin\theta$. The expressions obtained for coordinates and frequency are the following

$$
\begin{aligned}
q_1 &= A\cos\theta - \frac{5}{32}A^3\cos\theta + \frac{1}{16}A^3\cos 3\theta + \frac{629}{6144}A^5\cos\theta - \frac{179}{3072}A^5\cos 3\theta \\
&\quad - \frac{25}{1024}A^5\cos 5\theta - \frac{55577}{589824}A^7\cos\theta + \frac{4103}{65536}A^7\cos 3\theta + \frac{21971}{589824}A^7\cos 5\theta \\
&\quad - \frac{1025}{147456}A^7\cos 7\theta \\
q_2 &= A\sin\theta - \frac{5}{32}A^3\sin\theta - \frac{1}{16}A^3\sin 3\theta + \frac{629}{6144}A^5\sin\theta + \frac{179}{3072}A^5\sin 3\theta \\
&\quad - \frac{25}{1024}A^5\sin 5\theta - \frac{55577}{589824}A^7\sin\theta - \frac{4103}{65536}A^7\sin 3\theta + \frac{21971}{589824}A^7\sin 5\theta \\
&\quad + \frac{1025}{147456}A^7\sin 7\theta \\
\dot{\theta} &= 1 + \frac{1}{8}A^2 - \frac{3}{256}A^4 - \frac{3}{2048}A^6
\end{aligned}
\tag{3.56}
$$

For $E \approx 1/8$ comparisons are made with numerical integration. With initial conditions of $q_1 = 0.34, p_1 = 0, q_2 = 0, p_2 = 0.34$. q_1 against q_2 is plotted along numerical solution in Figure 3.10. Also, time dependence of q_1 and q_2 is shown in Figure 3.11 and Figure 3.12 respectively. Up to timescale of 50 very good agreement is achieved with numerical one especially for the coordinate q_1. The results as follows:

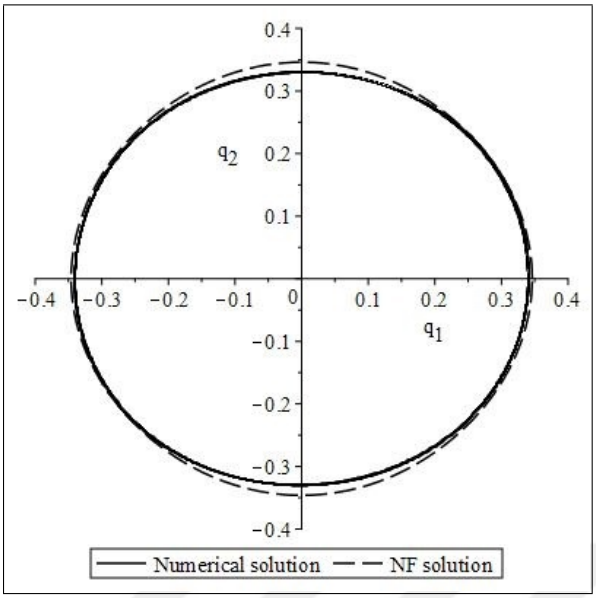

Figure 3.10. Comparison of numerical and normal form solution for $E \approx 0.125$

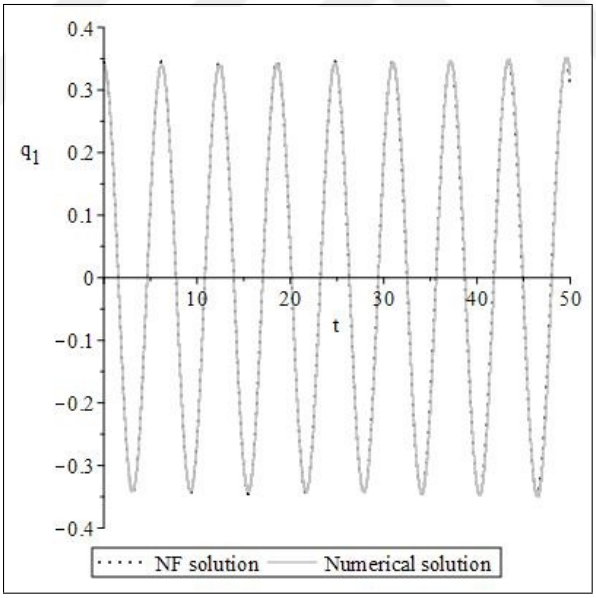

Figure 3.11. Comparison of numerical and normal form solution for $E \approx 0.125$

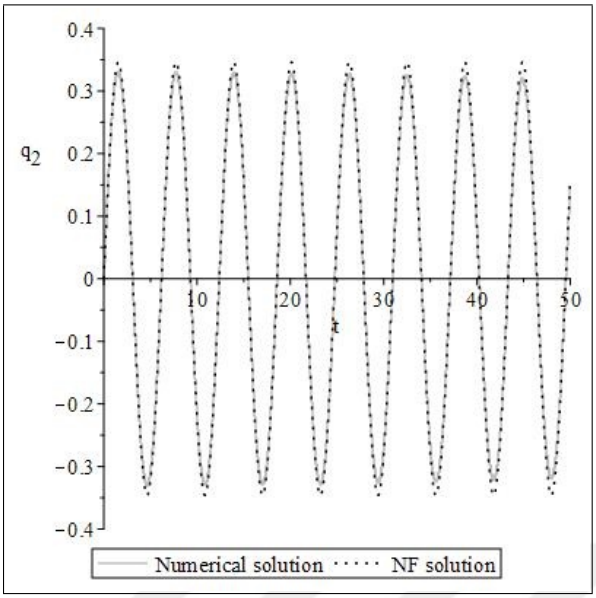

Figure 3.12. Comparison of numerical and normal form solution for $E \approx 0.125$

The normal form solutions obtained for periodic orbits with the use of Lie Transform method have similar structure with those of [41, 42] where the authors use Poincaré-Lindstedt method and Poincaré normal forms respectively to obtain periodic solutions of Hamiltonian systems.

3.4.2. Periodic Solutions for System (2.21)

With the same procedure applied above the periodic solutions are obtained for system (2.21) also. Starting from axial orbits, for $J_2 = 0$ the expression of K is given as;

$$K = J_1 + \frac{3}{16}J_1^2 - \frac{17}{256}J_1^3 + \frac{375}{8192}J_1^4 \tag{3.57}$$

Then periodic solution representing q_1 and the frequency is given by;

$$\begin{aligned} q_1 = {} & A\cos\theta - \frac{3}{32}A^3\cos\theta + \frac{1}{64}A^3\cos 3\theta + \frac{303}{8192}A^5\cos\theta - \frac{39}{4096}A^5\cos 3\theta \\ & - \frac{1}{4096}A^5\cos 5\theta - \frac{1263}{65536}A^7\cos\theta + \frac{3219}{524288}A^7\cos 3\theta - \frac{73}{262144}A^7\cos 5\theta \\ & + \frac{1}{262144}A^7\cos 7\theta \end{aligned} \tag{3.58}$$

$$\dot{\theta} = 1 + \frac{3}{16}A^2 - \frac{51}{1024}A^4 + \frac{375}{16384}A^6$$

The solutions are compared with numerical ones with an initial conditions of $q_1 = 0.70, p_1 = 0.0$ which correspond to an energy of $E = 0.275$. The comparisons of solutions are shown below

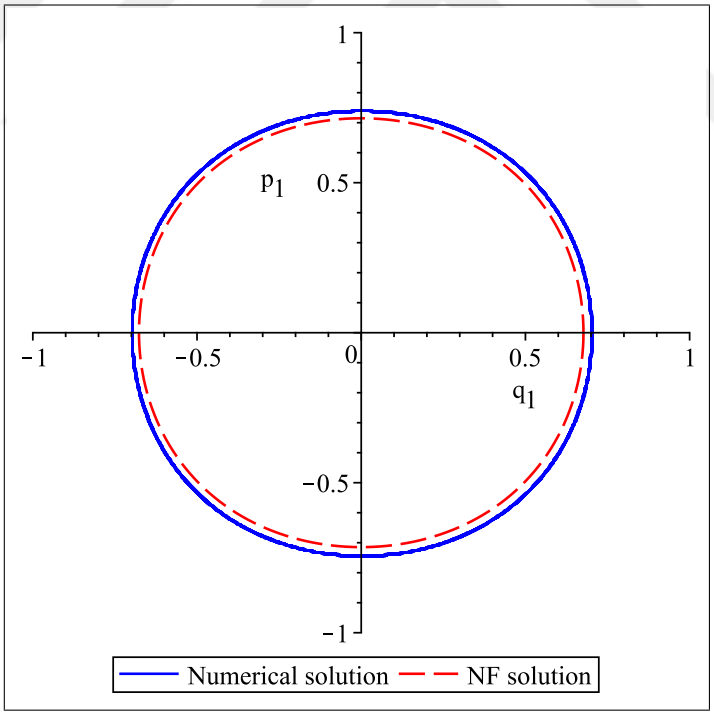

Figure 3.13. Comparison of numerical and normal form solution for $E = 0.275$

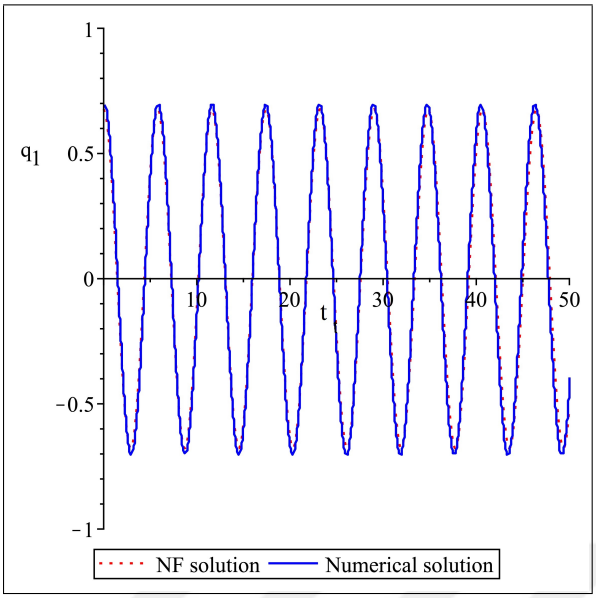

Figure 3.14. Comparison of numerical and normal form solution for $E = 0.275$

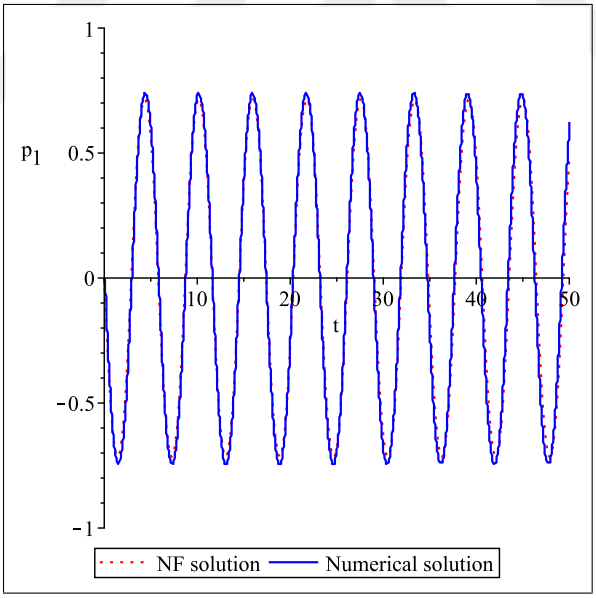

Figure 3.15. Comparison of numerical and normal form solution for $E = 0.275$

For the oblique solutions $q_1 = \pm q_2$ the expressions for normalized Hamiltonian and periodic

solutions are the following :

$$
\begin{aligned}
K =& 2J_1 + \frac{9}{8}J_1^2 - \frac{153}{128}J_1^3 + \frac{10125}{4096}J_1^4 \\
q_1 =& A\cos\theta - \frac{9}{32}A^3\cos\theta + \frac{3}{64}A^3\cos 3\theta + \frac{2727}{8192}A^5\cos\theta - \frac{351}{4096}A^5\cos 3\theta \\
&+ \frac{9}{4096}A^5\cos 5\theta - \frac{34101}{65536}A^7\cos\theta + \frac{86913}{524288}A^7\cos 3\theta - \frac{1971}{262144}A^7\cos 5\theta \\
&+ \frac{27}{262144}A^7\cos 7\theta \\
\dot{\theta} =& 2 + \frac{9}{8}A^2 - \frac{459}{512}A^4 + \frac{10125}{8192}A^6
\end{aligned}
\tag{3.59}
$$

The comparisons are made with numerical solutions of initial conditions of $q_1 = 0.70, p_1 = 0.0$ with an energy of $E = 0.67$.

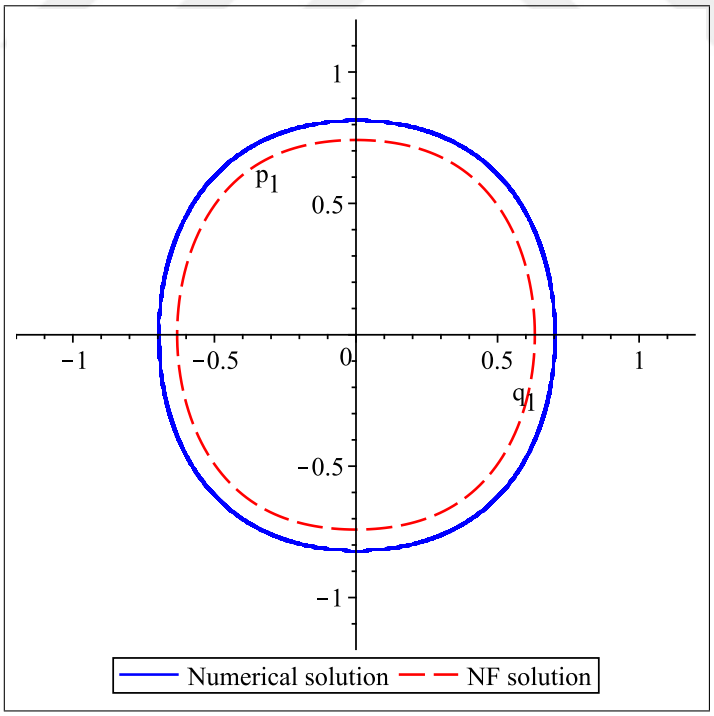

Figure 3.16. Comparison of numerical and normal form solution for $E = 0.67$

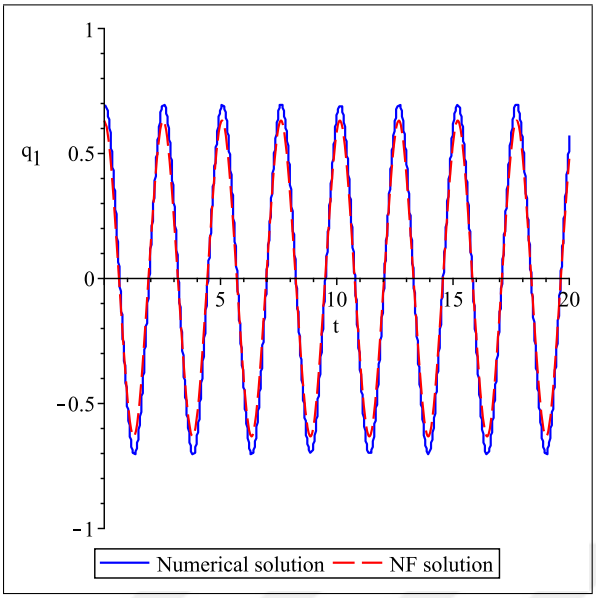

Figure 3.17. Comparison of numerical and normal form solution for $E = 0.67$

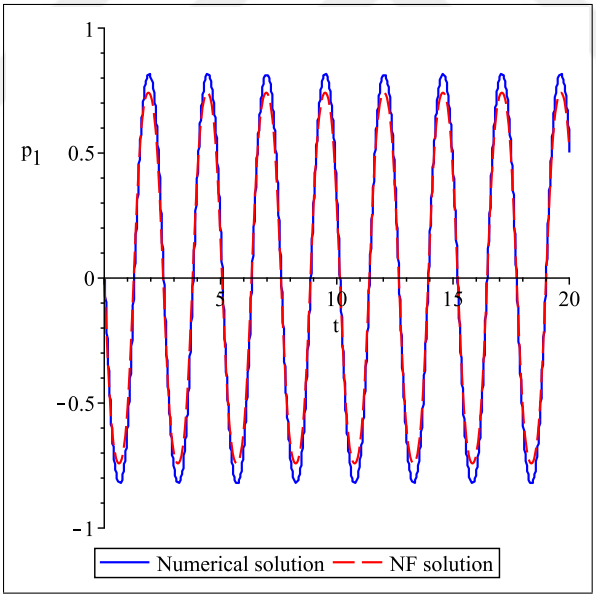

Figure 3.18. Comparison of numerical and normal form solution for $E = 0.67$

On the other hand for loop orbits the obtained solutions are the following

$$\begin{aligned} K =& J_1 + J_2 + \frac{3}{16}J_1^2 + \frac{3}{16}J_2^2 + \frac{1}{4}J_1J_2 - \frac{17}{256}J_1^3 - \frac{17}{256}J_2^3 - \frac{1}{8}J_1^2J_2 - \frac{1}{8}J_2^2J_1 \\ &+ \frac{375}{8192}J_1^4 + \frac{375}{8192}J_2^4 + \frac{473}{4096}J_1^3J_2 + \frac{473}{4096}J_2^3J_1 + \frac{73}{512}J_1^2J_2^2 \end{aligned} \tag{3.60}$$

$$\begin{aligned} q_1 =& A\cos\theta - \frac{1}{4}A^3\cos\theta + \frac{5}{64}A^3\cos 3\theta + \frac{6625}{24576}A^5\cos\theta - \frac{197}{1536}A^5\cos 3\theta \\ &- \frac{19}{1024}A^5\cos 5\theta - \frac{114917}{294912}A^7\cos\theta + \frac{117793}{524288}A^7\cos 3\theta + \frac{33391}{589824}A^7\cos 5\theta \\ &- \frac{8897}{1179648}A^7\cos 7\theta \\ q_2 =& A\sin\theta - \frac{1}{4}A^3\sin\theta - \frac{5}{64}A^3\sin 3\theta + \frac{6625}{24576}A^5\sin\theta + \frac{197}{1536}A^5\sin 3\theta \\ &- \frac{19}{1024}A^5\sin 5\theta - \frac{114917}{294912}A^7\sin\theta - \frac{117793}{524288}A^7\sin 3\theta + \frac{33391}{589824}A^7\sin 5\theta \\ &+ \frac{8897}{1179648}A^7\sin 7\theta \\ \dot{\theta} =& 1 + \frac{5}{16}A^2 - \frac{147}{1024}A^4 + \frac{1905}{16384}A^6 \end{aligned} \tag{3.61}$$

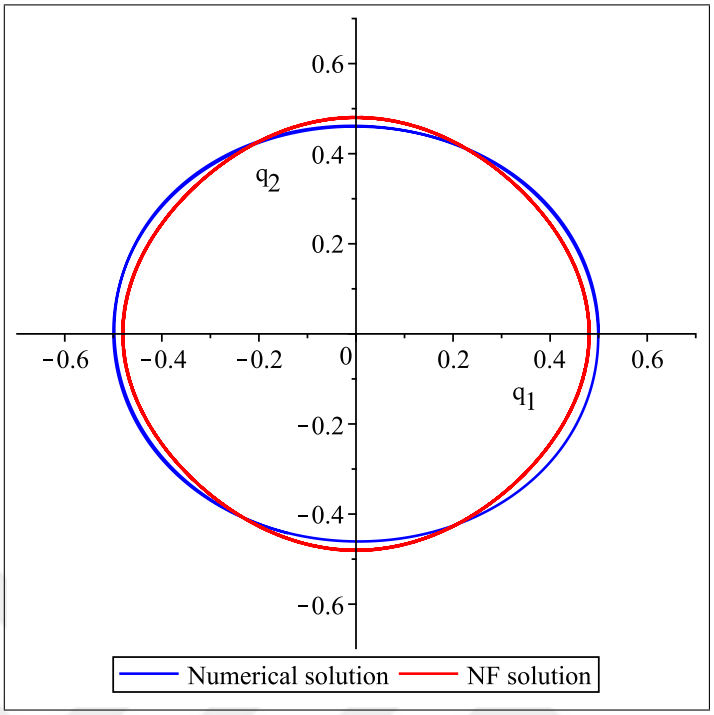

Figure 3.19. Comparison of numerical and normal form solution for $E = 0.257$

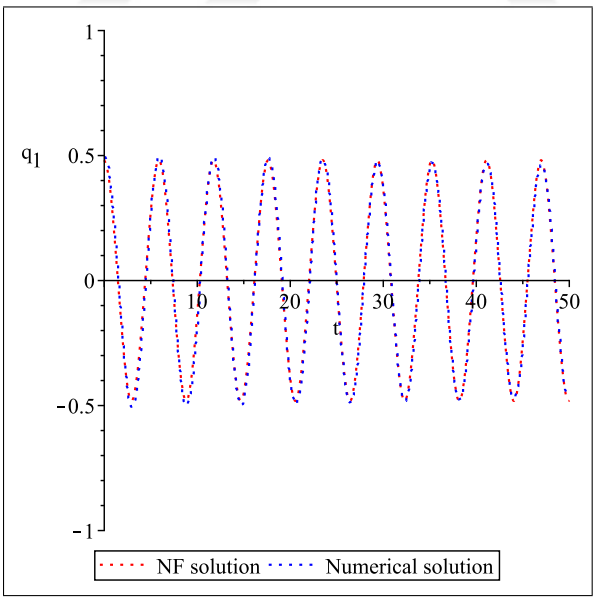

Figure 3.20. Comparison of numerical and normal form solution for $E = 0.257$

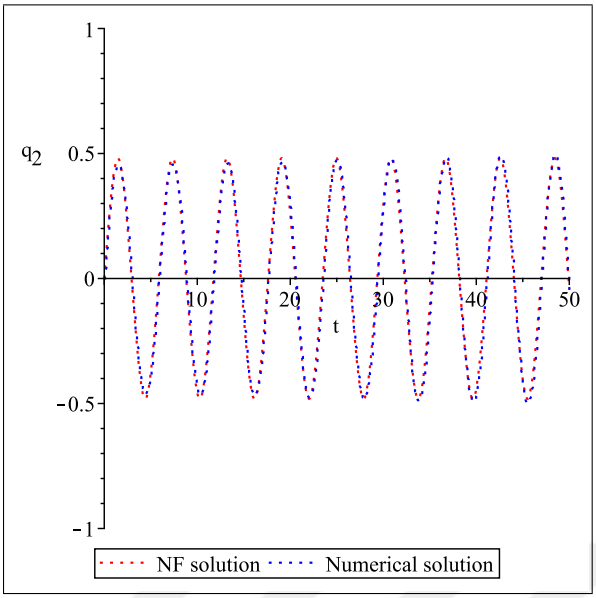

Figure 3.21. Comparison of numerical and normal form solution for $E = 0.257$

Regarding comparisons it can be concluded that good agreement is achieved, especially for lower energies. It is also important to note that approximation in oblique solutions get more deviated from numerical ones. This is mostly due to increasing coefficient of nonlinear term in the system, secondly higher energies remove the periodicity of motions, and system rather tend towards quasiperiodic and chaotic motion. It is obvious that the solutions obtained with Inverse Transforms are compatible with respect to numerical solutions although the obtained series do not converge. Better approximations could be obtained by including higher order terms in series.

3.5. POINCARÉ SECTIONS AND LEVEL CURVES OF APPROXIMATE INTEGRALS

The construction of convergent series for approximate integrals[43, 44] is important issue for usefulness of those integrals. Asymptotic behavior of these series that give rise the convergence depends on truncation order. For higher order of truncations, the series turn out to be divergent, so there exist an optimal truncation order where the variation of the truncated integral along particular orbit of the system is minimal [36]. It is expected that the

level curves generated by the approximate integrals are give clues of P.S.S. in the periodic and quasiperiodic regime.

3.5.1. Poincaré Sections for System (2.15)

Before numerical comparison of integrals and P.S.S, time dependence of the truncated integrals are taken into account, as in section 3.3.1 4^{th} order truncated integral has the least fluctuation and seems almost constant for this particular system. So we choose the 4^{th} order approximate integral as suitable to work with. In order to make a comparison between the analytical results for the approximate integrals, Poincaré sections are plotted in $q_1 - p_1$ axis for $q_2 = 0$. On the other hand theoretical invariant curves are derived using equation (23).

$$p_2^2 = 2E - p_1^2 - q_1^2 \tag{3.62}$$

Then for $q_2 = 0$ the expressions for the integrals become

$$I = 2E - \frac{1}{16}(q_1^2 + 3p_1^2)(2E - p_1^2 - q_1^2) + \cdots \tag{3.63}$$

The elliptical fixed points of the Poincaré Sections correspond to maxima or minima of the integral on the other hand hyperbolic fixed points correspond to saddle points of the integral. For our case five fixed points on the Poincaré Section appeared. Three of them correspond to elliptical fixed points which are at the center, below and above the center, and two hyperbolic fixed points which are left and right side of the center in the Poincaré plot. For energy level $E = 0.4$ up to nearly $E = 1$ there is a good agreement between approximate and numerical solutions which is depicted in Figure 3.22 and Figure 3.23, but after $E = 1$ stochastic regions [45] appear in Poincaré sections from those unstable hyperbolic fixed points which is shown in Figure 3.24 and Figure 3.25.

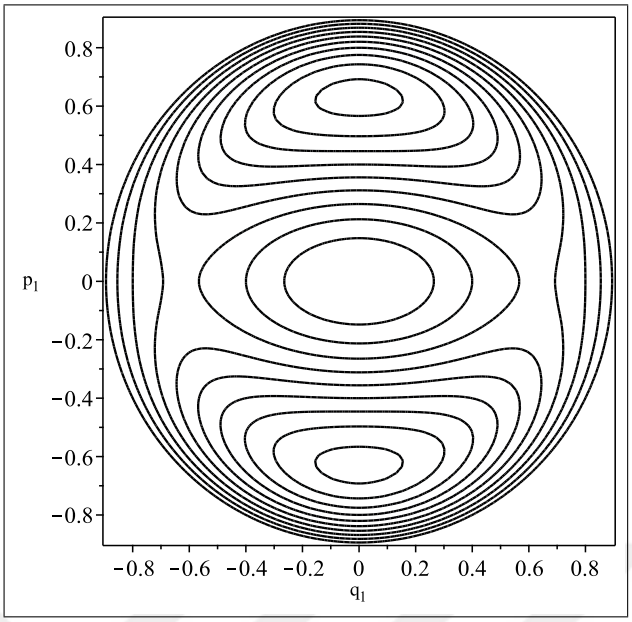

Figure 3.22. Level curves of approximate integral with $E = 0.4$

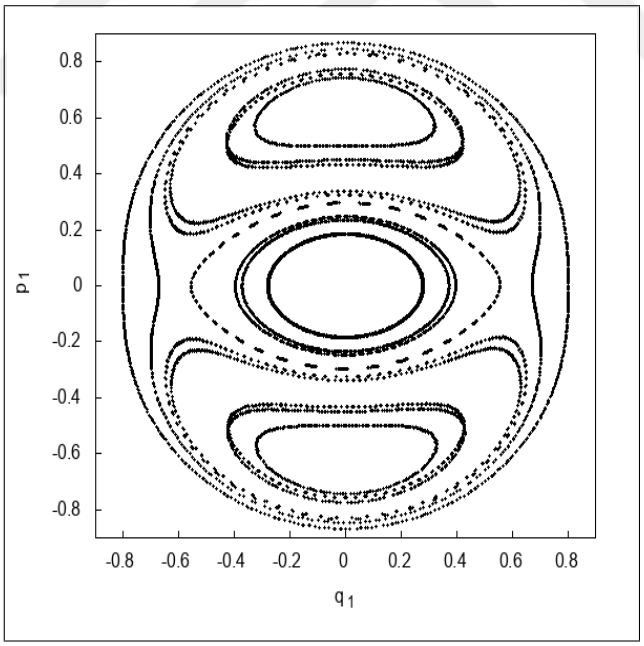

Figure 3.23. Poincaré surface section with $E = 0.4$

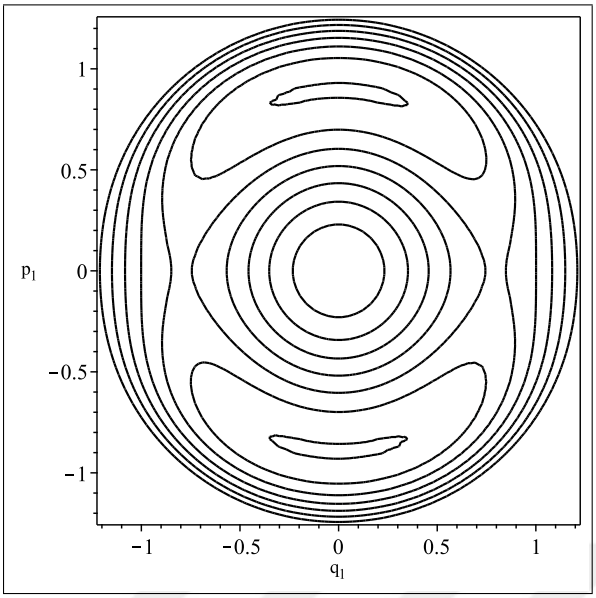

Figure 3.24. Level curves of approximate integral of order 4 with $E = 1.25$

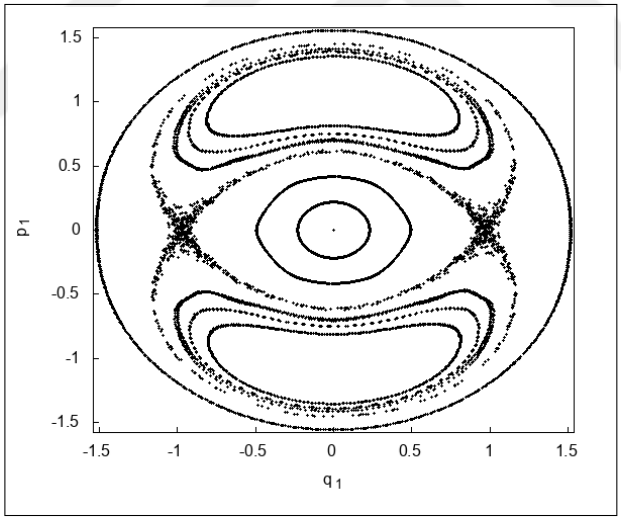

Figure 3.25. Poincaré surface section with $E = 1.25$

3.5.2. Poincaré Sections for System (2.21)

The above procedure is carried out for system 2.21. Again Poincaré sections are plotted in $q_1 - p_1$ axis for $q_2 = 0$ surface. Unlike system 2.15 this Hamiltonian and corresponding integral depend on parameter p. For fixed energy and varying p, comparisons are done

between P.S.S and invariant curves generated by truncated integral. For the expression of Integral, 4^{th} order truncated integral is chosen. In general, good agreement is achieved between P.S.S. and invariant curves of Integrals. Some of the important results are shown below.

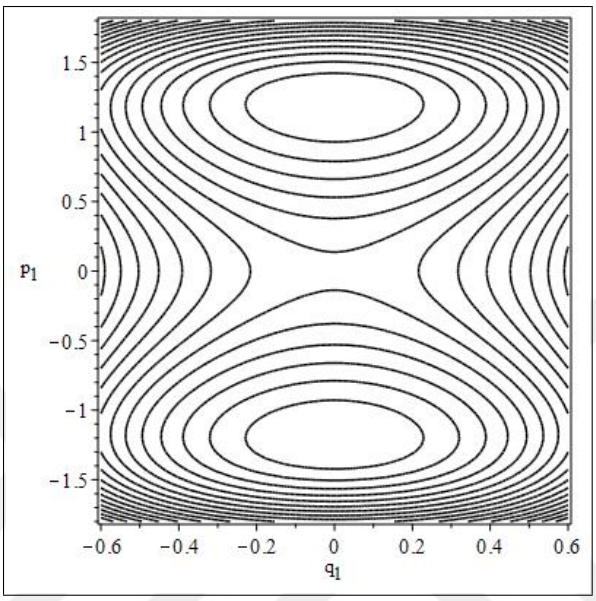

Figure 3.26. Level curves of approximate integral with $E = 2$

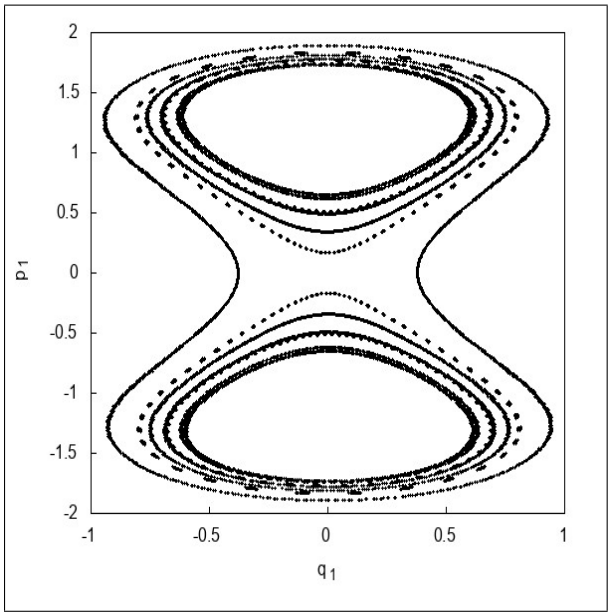

Figure 3.27. Level curves of approximate integral with $E = 2$

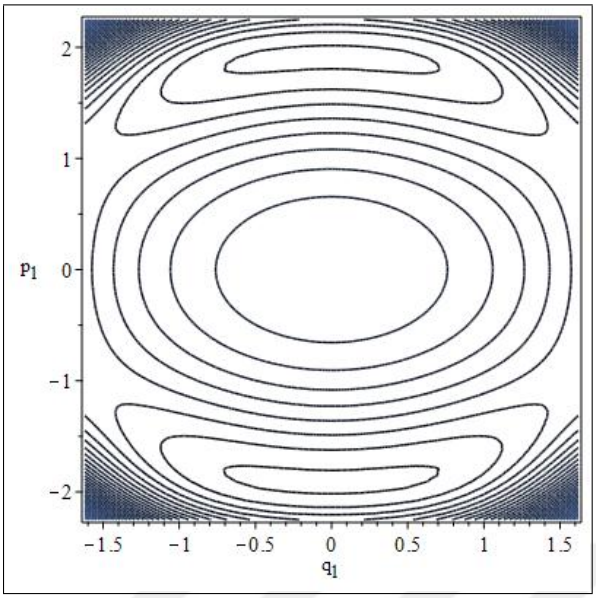

Figure 3.28. Level curves of approximate integral with $E = 2$

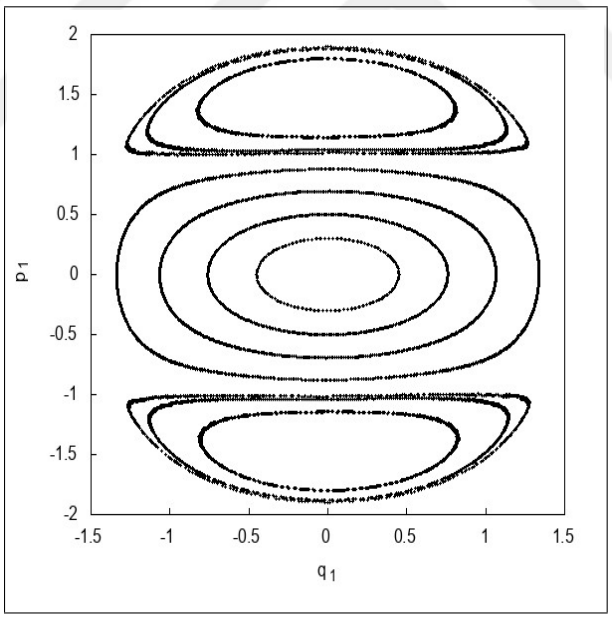

Figure 3.29. Level curves of approximate integral with $E = 2$

While Figure 3.26 and Figure 3.27 are plotted for $p = 1/8$, Figure 3.28 and Figure 3.29 are plotted for $p = 1/20$. It can be seen that varying p is producing different KAM curves. However, integrals are able to mimic these curves. Keeping energy constant, further decrease in p yields similar diagrams as in Figure 3.28 with small differences. Increasing p yields periodic orbits in P.S.S, which can be simulated again with those integrals.

4. CONCLUSIONS

Dynamical properties of Yang Mills mechanics are essential for better understanding of particle physics and gauge theories. In this respect this thesis concentrated on classical dynamics of homogeneous Yang Mills fields and Higgs coupling. First part of the work is devoted to determine complex behavior of the Yang Mills fields with symmetry group of SU(2). Even if considering simplest case of the fields, in which they are only time dependent, chaotic dynamics appear in 2 degrees of freedom. Then Higgs mechanism is considered with two different coupling mechanism to Yang Mills fields. It is numerically verified that Higgs field is responsible to stabilize the chaotic nature of Yang Mills fields and chaos order transtions take place instead of purely chaotic motion. This is essentially due to the fact that in the first model considered with specified field configurations, the Higgs mechanism generates harmonic terms and for small energies the motion is dominated by harmonic oscillator terms. With this knowledge, harmonic terms are included in the second mechanical model in which Hamiltonian involves x^4 and y^4 terms beside the well-known x^2y^2 potential. The additional terms dramatically change the dynamics of the system, and it is numerically verified that while keeping the energy of the system constant, increasing the coefficient of harmonic terms stabilize chaotic behaviour of system.

The other part of the work is devoted to obtaining analytical results using perturbation method. The motivation behind this is mostly the work introduced by Gustavson to construct formal integrals in the famous Henon Heiles system. To obtain the analytical results Lie Transform method is used instead of other traditional approaches. Especially the method introduced by Dragt and Finn is considered to take the advantage of obtaining approximate integrals while normalizing the Hamiltonian, however one drawback of the method is that one needs the inverse transformations to obtain original solutions. With the use of symbolic software, the calculations can be implemented without any problem, but for higher order perturbations one needs efficient algorithms, since they use greater memory and CPU time. Especially for small energies where system is dominated with periodic and quasiperiodic motions, the expressions yields good qualitative predictions on the dynamics appearing in phase portraits. After normalizing the Hamiltonian, it is more suitable to use action angle coordinates. To obtain periodic solutions one needs to get rid of resonant terms in the

expansions. This can be achieved in different ways and each of them is named with different families of periodic solutions. The expressions have same structure as they are series of trigonometric functions. Each of them is numerically tested and it can be concluded that the analytic expressions for coordinates and frequency are in good agreement up to a certain energy level. On the other hand, the analytical expressions for approximate integrals are used to simulate Poincaré sections. It is important to note that the series expansion for integrals may not converge. For this purpose, time dependence of integrals is analyzed, and the integrals are truncated with least fluctuation. The level curves generated by those integrals are numerically tested with Poincaré sections and good agreement is obtained up to some energy. Beyond this energy KAM curves start to break and chaotic regions appear in the Poincaré section, those regions can not be simulated with approximate integrals. Throughout the thesis classical dynamics of Yang Mills mechanics is considered, however there is deep relation to quantum mechanical properties of Yang Mills fields[46]. The findings in this thesis can also be useful also in the quantum counterpart. With the use of quantum perturbation theory similar results can be obtained, this will enlighten the unknown parts of Yang Mills mechanics, and perhaps quantum normal forms can be constructed and quantum properties may become more tractable.

REFERENCES

1. Actor A. Classical solutions of SU (2) Yang-Mills theories. *Reviews of Modern Physics*. 1979;51(3):461.

2. Lakshmibala S, Bambah BA, Sriram MS, Mukku C. Classical gauge theories as dynamical systems-Regularity and chaos. *Pramana Journal of Physics*. 1997;48(2):617-35.

3. Wolf A, Swift JB, Swinney HL, Vastano JA. Determining Lyapunov exponents from a time series. *Physica D: Nonlinear Phenomena*. 1985;16(3):285-317.

4. Kasperczuk S. Integrability of the Yang-Mills hamiltonian system. *Celestial Mechanics and Dynamical Astronomy*. 1994;58(4):387-91.

5. Joy MP, Sabir M. Non-integrability of SU (2) Yang-Mills and Yang-Mills-Higgs systems. *Journal of Physics A: Mathematical and General*. 1989;22(23):5153-5160.

6. Matinyan SG, Savvidy GK, Ter-Arutyunyan-Savvidy NG. Classical Yang-Mills mechanics. nonlinear color oscillations. *Sov. Phys. JETP*.1981;80:830-8.

7. Kibble TW. Symmetry breaking in non-Abelian gauge theories. *Physical Review*. 1967;155(5):1554-1561.

8. Han M, Yu P. *Normal forms, Melnikov functions and bifurcations of limit cycles*. London: Springer Science and Business Media; 2012.

9. Belmonte C, Boccaletti D, Pucacco G. Approximate first integrals with the method of lie transform normalization. *Qualitative Theory of Dynamical Systems*. 2008;7(1):43-71.

10. Rand RH, Armbruster D. *Perturbation methods, bifurcation theory and computer algebra*. New York: Springer Science and Business Media; 2012.

11. Gaeta G. Reduction of Poincar normal forms. *Letters in Mathematical Physics*. 1997;42(2):103-14.

12. Broer H, Hoveijn I, Lunter G, Vegter G. *Bifurcations in Hamiltonian systems: computing singularities by Grbner bases*. New York: Springer; 2003.

13. Gustavson FG. On constructing formal integrals of a Hamiltonian system near an equilibrium point. *The Astronomical Journal*. 1966;71:670-686.

14. Ito H. Convergence of Birkhoff normal forms for integrable systems. *Commentarii Mathematici Helvetici*. 1989;64(1):412-61.

15. Mikram J, Zinoun F. Normal form methods for symbolic creation of approximate solutions of nonlinear dynamical systems. *Mathematics and Computers in Simulation*. 2001;57(3-5):253-89.

16. Broer HW, Sevryuk MB. Kam Theory: quasi-periodicity in dynamical systems. *Handbook of Dynamical Systems*. 2010;3(C):249-344.

17. Celletti A, Chierchia L. *KAM stability and celestial mechanics*. Rhode Island: American Mathematical Soc.; 2007.

18. Salasnich L. Chaos suppression in the SU (2) Yang-Mills-Higgs system. *Physical Review D*. 1995;52(10):6189-6191.

19. Bernstein J. Spontaneous symmetry breaking, gauge theories, the Higgs mechanism and all that. *Reviews of Modern Physics*. 1974;46(1):7-48.

20. Sergei M. *Chaos and gauge field theory*. New Jersey: World Scientific; 1995.

21. Magnitskii NA. Chaotic dynamics of homogeneous Yang-Mills Fields with two degrees of freedom. *Differential Equations*. 2009;45(12):1732-1737.

22. Rossler OE. An equation for hyperchaos. *Physics Letters A*. 1979;71(2-3):155-7.

23. Kapitaniak T, Maistrenko Y, Popovych S. Chaos-hyperchaos transition. *Physical Review E*. 2000;62(2):1972-1976.

24. Cary JR. Lie transform perturbation theory for Hamiltonian systems. *Physics Reports*. 1981;79(2):129-159.

25. Nayfeh AH. *Perturbation methods*.Weinheim: John Wiley and Sons; 2008.

26. Reichl L. *The transition to chaos: conservative classical systems and quantum manifestations*. New York: Springer Science and Business Media; 2013.

27. Duffy B, Chichka DF. Canonical Perturbation Theory for the Elliptic Restricted-Three-Body Problem. *Advances in the Astronautical Sciences*. 2012; 143(11):1267-1286.

28. Deprit A. Canonical transformations depending on a small parameter. *Celestial Mechanics*. 1969;1(1):12-30.

29. Dragt AJ, Finn JM. Lie series and invariant functions for analytic symplectic maps. *Journal of Mathematical Physics*. 1976;17(12):2215-27.

30. Koseleff PV. Comparison between Deprit and Dragt-Finn perturbation methods. *Celestial Mechanics and Dynamical Astronomy*. 1994;58(1):17-36.

31. Deruni B, Hacinliyan AS. Approximate integrals in YangMillsHiggs system using lie transforms. *Few-Body Systems*. 2019;60(1-4):74-89.

32. Contopoulos G. *Order and chaos in dynamical astronomy*. Athens: Springer Science and Business Media; 2013.

33. Verhulst F, Tuwankotta JM. Symmetry and resonance in Hamiltonian systems. *SIAM Journal on Applied Mathematics*. 2001;61(4):1369-85.

34. Boccaletti D, Pucacco G. *Theory of orbits: Perturbative and geometrical methods*. Rome: Springer Science and Business Media; 2013.

35. Kahn PB, Zarmi Y. *Nonlinear dynamics: exploration through normal forms*. New York: Courier Corporation; 2014.

36. Contopoulos G, Efthymiopoulos C, Giorgilli A. Non-convergence of formal integrals of motion. *Journal of Physics A: Mathematical and General*. 2003;36(32):8639-8660.

37. Mikram J, Zinoun F. Computation of normal forms of Hamiltonian systems in the presence of Poisson commuting integrals. *Numerical Algorithms*. 1999;21(1-4):287-310.

38. Murdock J. *Normal forms and unfoldings for local dynamical systems*. New York:Springer Science and Business Media; 2006.

39. Sanders JA, Verhulst F, Murdock JA. *Averaging methods in nonlinear dynamical systems*. New York: Springer; 2007.

40. Pucacco G, Boccaletti D, Belmonte C. Periodic orbits in the logarithmic potential. *Astronomy and Astrophysics*. 2008;489(3):1055-63.

41. Benbachir S. Symbolic research of the periodic solutions of the nonintegrable Hamiltonian system of Ollongren. *Numerical Algorithms*. 1999;21(1-4):57-77.

42. Edneral VF. Looking for periodic solutions of ode systems by the normal form method. *Differential equations with symbolic computation*. 2005:173-200.

43. Giorgilli A, Galgani L. Formal integrals for an autonomous Hamiltonian system near an equilibrium point. *Celestial Mechanics*. 1978;17(3):267-80.

44. Efthymiopoulos C. Formal integrals and Nekhoroshev stability in a mapping model for the Trojan asteroids. *Celestial Mechanics and Dynamical Astronomy*. 2005;92(1-3):29-52.

45. Lichtenberg AJ, Lieberman MA. *Regular and stochastic motion*. New York: Springer Science and Business Media; 2013.

46. Salasnich L. Quantum chaos in a YangMillsHiggs system. *Modern Physics Letters A*. 1997;12(20):1473-80.

APPENDIX A: RESULTS FOR SYSTEM (2.15)

The terms in the normalized Hamiltonian are given by

$$K_0 = \frac{{P_1}^2}{2} + \frac{{P_2}^2}{2} + \frac{{Q_1}^2}{2} + \frac{{Q_2}^2}{2}$$

$$K_2 = \frac{3{P_1}^2{P_2}^2}{16} + \frac{{P_1}^2{Q_2}^2}{16} + \frac{P_1P_2Q_1Q_2}{4} + \frac{{P_2}^2{Q_1}^2}{16} + \frac{3{Q_1}^2{Q_2}^2}{16}$$

$$\begin{aligned} K_4 = &-\frac{17\,{P_1}^2{P_2}^4}{512} - \frac{{P_2}^4{Q_1}^2}{512} - \frac{{P_1}^2{Q_2}^4}{512} - \frac{17\,{P_1}^4{P_2}^2}{512} - \frac{{P_1}^4{Q_2}^2}{512} \\ &- \frac{{P_2}^2{Q_1}^4}{512} - \frac{9\,{P_1}^2{P_2}^2{Q_2}^2}{256} - \frac{9\,{P_2}^2{Q_1}^2{Q_2}^2}{256} - \frac{9\,{P_1}^2{P_2}^2{Q_1}^2}{256} \\ &- \frac{9\,{P_1}^2{Q_1}^2{Q_2}^2}{256} - \frac{17\,{Q_1}^2{Q_2}^4}{512} - \frac{17\,{Q_1}^4{Q_2}^2}{512} - \frac{P_1{P_2}^3Q_1Q_2}{16} \\ &- \frac{P_1P_2Q_1{Q_2}^3}{16} - \frac{{P_1}^3P_2Q_1Q_2}{16} - \frac{P_1P_2{Q_1}^3Q_2}{16} \end{aligned}$$

$$\begin{aligned} K_6 = &\frac{57\,P_1P_2{Q_1}^5Q_2}{4096} + \frac{49\,{P_1}^3{P_2}^3Q_1Q_2}{512} + \frac{49\,P_1P_2{Q_1}^3{Q_2}^3}{512} \\ &+ \frac{57\,P_1{P_2}^5Q_1Q_2}{4096} + \frac{57\,P_1P_2Q_1{Q_2}^5}{4096} + \frac{57\,{P_1}^5P_2Q_1Q_2}{4096} \\ &+ \frac{17\,{P_1}^3P_2Q_1{Q_2}^3}{512} + \frac{123\,{P_1}^2{P_2}^2{Q_1}^2{Q_2}^2}{1024} + \frac{17\,P_1{P_2}^3{Q_1}^3Q_2}{512} \\ &+ \frac{57\,P_1{P_2}^3Q_1{Q_2}^3}{2048} + \frac{57\,{P_1}^3P_2{Q_1}^3Q_2}{2048} + \frac{125\,{P_1}^4{P_2}^4}{4096} + \frac{125\,{P_1}^2{P_2}^6}{16384} \\ &+ \frac{125\,{P_1}^6{P_2}^2}{16384} - \frac{7\,{P_2}^4{Q_1}^4}{4096} + \frac{11\,{P_2}^6{Q_1}^2}{16384} + \frac{11\,{P_2}^2{Q_1}^6}{16384} \\ &- \frac{7\,{P_1}^4{Q_2}^4}{4096} + \frac{11\,{P_1}^2{Q_2}^6}{16384} + \frac{11\,{P_1}^6{Q_2}^2}{16384} + \frac{125\,{Q_1}^6{Q_2}^2}{16384} \end{aligned}$$

$$+\frac{125\,{Q_1}^2{Q_2}^6}{16384}+\frac{125\,{Q_1}^4{Q_2}^4}{4096}+\frac{147\,{P_1}^2{P_2}^2{Q_1}^4}{16384}+\frac{261\,{P_1}^4{P_2}^2{Q_1}^2}{16384}$$

$$+\frac{27\,{P_1}^2{P_2}^4{Q_1}^2}{2048}+\frac{147\,{P_1}^2{P_2}^2{Q_2}^4}{16384}+\frac{27\,{P_1}^4{P_2}^2{Q_2}^2}{2048}+\frac{261\,{P_1}^2{P_2}^4{Q_2}^2}{16384} \tag{A.1}$$

$$+\frac{147\,{P_1}^4{Q_1}^2{Q_2}^2}{16384}+\frac{261\,{P_1}^2{Q_1}^4{Q_2}^2}{16384}+\frac{27\,{P_1}^2{Q_1}^2{Q_2}^4}{2048}$$

$$+\frac{147\,{P_2}^4{Q_1}^2{Q_2}^2}{16384}+\frac{27\,{P_2}^2{Q_1}^4{Q_2}^2}{2048}+\frac{261\,{P_2}^2{Q_1}^2{Q_2}^4}{16384}$$

The terms in the generating function are given by

$$g_1 = 0$$

$$g_2 = \frac{3\,{P_1}^2P_2Q_2}{32}+\frac{3\,P_1{P_2}^2Q_1}{32}+\frac{5\,P_1Q_1{Q_2}^2}{32}+\frac{5\,P_2{Q_1}^2Q_2}{32}$$

$$g_3 = 0$$

$$g_4 = -\frac{13\,P_1{P_2}^4Q_1}{768}-\frac{19\,P_1Q_1{Q_2}^4}{768}-\frac{13\,{P_1}^4P_2Q_2}{768}-\frac{19\,P_2{Q_1}^4Q_2}{768}$$

$$-\frac{13\,{P_1}^2{P_2}^3Q_2}{384}-\frac{5\,{P_1}^2P_2{Q_2}^3}{384}-\frac{5\,{P_2}^3{Q_1}^2Q_2}{384}-\frac{19\,P_2{Q_1}^2{Q_2}^3}{384}$$

$$-\frac{13\,{P_1}^3{P_2}^2Q_1}{384}-\frac{5\,{P_1}^3Q_1{Q_2}^2}{384}-\frac{5\,P_1{P_2}^2{Q_1}^3}{384}-\frac{19\,P_1{Q_1}^3{Q_2}^2}{384}$$

$$-\frac{7\,P_1{P_2}^2Q_1{Q_2}^2}{64}-\frac{7\,{P_1}^2P_2{Q_1}^2Q_2}{64}$$

$$g_5 = 0$$

$$
\begin{aligned}
g_6 = {} & \frac{407\,{P_1}^3{P_2}^2Q_1{Q_2}^2}{4096} + \frac{15679\,P_1{P_2}^4Q_1{Q_2}^2}{589824} + \frac{407\,{P_1}^2{P_2}^3{Q_1}^2Q_2}{4096} \\
& + \frac{15679\,{P_1}^4P_2{Q_1}^2Q_2}{589824} + \frac{441\,P_1{P_2}^2{Q_1}^3{Q_2}^2}{4096} + \frac{20929\,P_1{P_2}^2Q_1{Q_2}^4}{589824} \\
& + \frac{441\,{P_1}^2P_2{Q_1}^2{Q_2}^3}{4096} + \frac{20929\,{P_1}^2P_2{Q_1}^4Q_2}{589824} + \frac{2749\,P_1{P_2}^2{Q_1}^5}{589824} \\
& + \frac{4709\,{P_1}^3{P_2}^2{Q_1}^3}{294912} - \frac{121\,P_1{P_2}^4{Q_1}^3}{24576} + \frac{211\,{P_1}^3{P_2}^4Q_1}{8192} \\
& + \frac{3773\,{P_1}^5{P_2}^2Q_1}{589824} + \frac{3823\,P_1{P_2}^6Q_1}{589824} + \frac{4709\,{P_1}^2{P_2}^3{Q_2}^3}{294912} + \frac{3823\,{P_1}^6P_2Q_2}{589824} \\
& - \frac{121\,{P_1}^4P_2{Q_2}^3}{24576} + \frac{211\,{P_1}^4{P_2}^3Q_2}{8192} + \frac{2749\,{P_1}^2P_2{Q_2}^5}{589824} + \frac{3773\,{P_1}^2{P_2}^5Q_2}{589824} \\
& + \frac{3419\,{P_1}^3{Q_1}^3{Q_2}^2}{294912} + \frac{8003\,P_1{Q_1}^5{Q_2}^2}{589824} + \frac{4369\,P_1Q_1{Q_2}^6}{589824} - \frac{103\,{P_1}^3Q_1{Q_2}^4}{24576} \\
& + \frac{2755\,{P_1}^5Q_1{Q_2}^2}{589824} + \frac{1031\,P_1{Q_1}^3{Q_2}^4}{24576} - \frac{103\,{P_2}^3{Q_1}^4Q_2}{24576} + \frac{3419\,{P_2}^3{Q_1}^2{Q_2}^3}{294912} \\
& + \frac{8003\,P_2{Q_1}^2{Q_2}^5}{589824} + \frac{1031\,P_2{Q_1}^4{Q_2}^3}{24576} + \frac{4369\,P_2{Q_1}^6Q_2}{589824} + \frac{2755\,{P_2}^5{Q_1}^2Q_2}{589824}
\end{aligned}
$$

$$
I_0 = \frac{{p_1}^2}{2} + \frac{{q_1}^2}{2} + \frac{{p_2}^2}{2} + \frac{{q_2}^2}{2}
$$

$$
I_2 = -\frac{3{p_1}^2{p_2}^2}{16} - \frac{{p_1}^2{q_2}^2}{16} - \frac{p_1p_2q_1q_2}{4} - \frac{{p_2}^2{q_1}^2}{16} + \frac{5\,{q_1}^2{q_2}^2}{16}
\tag{A.2}
$$

$$
\begin{aligned}
I_4 = {} & \frac{35\,{p_1}^2{p_2}^4}{512} - \frac{5\,{p_2}^4{q_1}^2}{512} + \frac{11\,{p_1}^2{q_2}^4}{512} + \frac{35\,{p_1}^4{p_2}^2}{512} - \frac{5\,{p_1}^4{q_2}^2}{512} \\
& + \frac{11\,{p_2}^2{q_1}^4}{512} + \frac{15\,{p_1}^2{p_2}^2{q_2}^2}{256} + \frac{15\,{p_2}^2{q_1}^2{q_2}^2}{256} + \frac{15\,{p_1}^2{p_2}^2{q_1}^2}{256} \\
& + \frac{15\,{p_1}^2{q_1}^2{q_2}^2}{256} - \frac{13\,{q_1}^2{q_2}^4}{512} - \frac{13\,{q_1}^4{q_2}^2}{512} + \frac{5\,p_1{p_2}^3q_1q_2}{32} + \frac{p_1p_2q_1{q_2}^3}{32} \\
& + \frac{5\,{p_1}^3p_2q_1q_2}{32} + \frac{p_1p_2{q_1}^3q_2}{32}
\end{aligned}
$$

$$
\begin{aligned}
I_6 = {} & -\frac{275\,p_1p_2{q_1}^5q_2}{12288} - \frac{175\,{p_1}^3{p_2}^3q_1q_2}{512} - \frac{15\,p_1p_2{q_1}^3{q_2}^3}{512} - \frac{595\,p_1{p_2}^5q_1q_2}{12288} \\
& - \frac{275\,p_1p_2q_1{q_2}^5}{12288} - \frac{595\,{p_1}^5p_2q_1q_2}{12288} - \frac{35\,{p_1}^3p_2q_1{q_2}^3}{512} - \frac{315\,{p_1}^2{p_2}^2{q_1}^2{q_2}^2}{1024} \\
& - \frac{35\,p_1{p_2}^3{q_1}^3q_2}{512} - \frac{105\,p_1{p_2}^3q_1{q_2}^3}{2048} - \frac{105\,{p_1}^3p_2{q_1}^3q_2}{2048} - \frac{1645\,{p_1}^2{p_2}^2{q_1}^4}{49152} \\
& - \frac{2275\,{p_1}^4{p_2}^2{q_1}^2}{49152} - \frac{35\,{p_1}^2{p_2}^4{q_1}^2}{2048} - \frac{1645\,{p_1}^2{p_2}^2{q_2}^4}{49152} - \frac{35\,{p_1}^4{p_2}^2{q_2}^2}{2048} \\
& - \frac{2275\,{p_1}^2{p_2}^4{q_2}^2}{49152} - \frac{1085\,{p_1}^4{q_1}^2{q_2}^2}{49152} + \frac{205\,{p_1}^2{q_1}^4{q_2}^2}{49152} - \frac{75\,{p_1}^2{q_1}^2{q_2}^4}{2048} \\
& - \frac{1085\,{p_2}^4{q_1}^2{q_2}^2}{49152} - \frac{75\,{p_2}^2{q_1}^4{q_2}^2}{2048} + \frac{205\,{p_2}^2{q_1}^2{q_2}^4}{49152} - \frac{385\,{p_1}^2{p_2}^6}{16384} \\
& - \frac{385\,{p_1}^6{p_2}^2}{16384} - \frac{385\,{p_1}^4{p_2}^4}{4096} - \frac{365\,{p_2}^2{q_1}^6}{49152} + \frac{35\,{p_2}^6{q_1}^2}{49152} \\
& + \frac{35\,{p_2}^4{q_1}^4}{4096} + \frac{35\,{p_1}^6{q_2}^2}{49152} - \frac{365\,{p_1}^2{q_2}^6}{49152} + \frac{35\,{p_1}^4{q_2}^4}{4096} \\
& + \frac{47\,{q_1}^6{q_2}^2}{16384} + \frac{47\,{q_1}^2{q_2}^6}{16384} + \frac{47\,{q_1}^4{q_2}^4}{4096}
\end{aligned}
\tag{A.3}
$$

APPENDIX B: REDUCE PROGRAM FOR GENERATING VARIATIONAL EQUATIONS

This program generates the variational equations needed for the calculation of Lyapunov exponents in the Wolf algorithm which is given in the next appendix.

```
operator aa,v,y;
Yang-Mills-Higgs system equations
n:=4;
v(1):=y(3);
v(2):=y(4);
v(3):=-a**2*y(1)-y(1)*y(2)**2;
v(4):=-a**2*y(2)-y(1)**2*y(2);



nd:=n**2+n;
for j:=1:n do
for k:=1:n do
aa(j,k):=df(v(j),y(k));
for i:=1:n do
for k:=1:n do
v(i+n*k):=for j1:=1:n sum aa(k,j1)*y(n*j1+i);



load package gentran;
load package scope;
GENTRANLANG!* := FORTRAN
FORTLINELEN!* :=72;
on fort;
off period;
```

```
off getdecs;
off gendecs;
out”wolf.rf”;
write ” subroutine FCN(t,y,v) ”
write ” implicit real*8(a-h,o-z)”;
write ”* subroutine for wolf integration”
write ” dimension y(20),v(20) ”
for i:=1:nd do write v(i):=v(i)
write ” RETURN”
write ” END”
SHUT”wolf.rf”;
;end;;
```

APPENDIX C: FORTRAN PROGRAM FOR CALCULATION OF LYAPUNOV EXPONENT SPECTRUM USING THE WOLF ALGORITHM

```
Program liapode
implicit real*8(a-h,o-z)
N = No of nonlnear equations, NN= total No of equations
PARAMETER (N =4)
PARAMETER (NN=20)
NNN=No of divisions in the square interval
INTEGER NNN,KKK
common /params/ p,g
FOR THE NUM-REC INTEGRATOR
DIMENSION Y(NN),ZNORM(N),GSC(N),CUM(N),YPRIME(NN),YSCAL(NN)
LGX(N)= Sum of the Nth Lyapunov exponents
pi,pf,gi,gf=initial value of p, final value of p, initial value of g, final value of g of the square interval
REAL LGX(N),pi,pf,gi,gf
EXTERNAL FCN,RKQC
open(18, file='traj.dat', status='unknown')
open(19, file='liap.dat', status='unknown')
open(258, file='liapmax.dat', status='unknown')
INTEGRATION TOLERANCE, NO OF INTEGRATION STEPS,
TIME PER STEP, AND I/O RATE
STTOL=0
tol=0.00001d0
NNN=50
KKK=10
nstep=20000
stpsze=0.01d0
```

```
io=1
pi=0.1d0
pf=10d0
gi=0d0
gf=1d0
Do-loops for iteration of p and g
DO 251 JJ=0,NNN
p=pi+(pf-pi)*JJ/NNN
DO 252 KK=0,KKK
g=gi+(gf-gi)*KK/KKK
INITIAL CONDITIONS FOR NONLINEAR SYSTEM
Y(1)=0.1 D0
Y(2)=0.2 D0
Y(3)=0.1 D0
Y(4)=0.2 D0
INITIAL CONDITIONS FOR LINEAR SYSTEM (ORTHONORMAL FRAME)
DO 10 I=N+1,NN
10 Y(I)=0
DO 20 I=1,N
Y((N+1)*I)=1.0 D0
CUM(I)=0
LGX(I)=0
20 continue
Initialization for integration
NEQ=NN
X=0.0 D0
IND=1
DO 100 I=1,NSTEP
XEND=STPSZE*FLOAT(I)
Call any ODE Integrator - This is an IMSL routine
in the original
```

```
CALL DVERK(NEQ,FCN,X,Y,XEND,TOL,IND,C,NEQ,W,IER)
replaced by a Numerical Recipes routine
CALL RKQC(Y,YPRIME,NEQ,X,STPSZE,TOL,YSCAL,HDID,HNEXT,FCN)
CALL ODEINT(Y,NEQ,X,XEND,TOL,STPSZE,STTOL,NOK,NBAD,FCN,RKQC)
X=XEND


Construct a new orthonormal basis by Gram-Schmidt method
Normalize first vector


ZNORM(1)=0.0
DO 30 J=1,N
30 ZNORM(1)=ZNORM(1)+Y(N*J+1)**2
ZNORM(1)=SQRT(ZNORM(1))
DO 40 J=1,N
40 Y(N*J+1)=Y(N*J+1)/ZNORM(1)
GENERATE THE NEW ORTHONORMAL SET OF VECTORS
DO 80 J=2,N
GENERATE J-1 GSR COEFFICIENTS
DO 50 K=1,J-1
GSC(K)=0.0
DO 50 L=1,N
GSC(K)=GSC(K)+Y(N*L+J)*Y(N*L+K)
50 CONTINUE
CONSTRUCT A NEW VECTOR
DO 60 K=1,N
DO 60 L=1,J-1
Y(N*K+J)=Y(N*K+J)-GSC(L)*Y(N*K+L)
60 CONTINUE
CALCULATE THE VECTOR'S NORM
ZNORM(J)=0.0 D0
```

```
DO 70 K=1,N
ZNORM(J)=ZNORM(J)+Y(N*K+J)**2
70 CONTINUE
ZNORM(J)=SQRT(ZNORM(J))
NORMALIZE THE NEW VECTOR
DO 80 K=1,N
Y(N*K+J)=Y(N*K+J)/ZNORM(J)
80 CONTINUE
UPDATE RUNNING VECTOR MAGNITUDES
DO 90 K=1,N
90 CUM(K)=CUM(K)+DLOG(ZNORM(K))/DLOG(2.0D0)
NORMALIZE EXPONENT AND PRINT EVERY IO ITERATIONS
IF(MOD(I,IO).EQ.0) THEN
WRITE(*,126) X,(CUM(K)/X,K=1,N)
126 Format('X= ',f12.7,' LE = ',4(F13.7,1x))
139 FORMAT(f12.7,4(F13.7,1x))
ENDIF
DO 201 K=1,N
201 LGX(K)=LGX(K)+CUM(K)/X
138 FORMAT(1X,F10.2, 4(1X,F14.4))
100 CONTINUE
```

Write the calculated maximum Lyapunov exponent in a data file as a function of g and p

```
WRITE(258,250)p,g,(LGX(K)/NSTEP,K=1,N)
250 FORMAT(f12.7,f12.7,4(F13.7,1x))
252 CONTINUE
251 CONTINUE
CLOSE(258)
STOP
END
```

USER DEFINED ROUTINE CALLED BY NUMERICAL RECIPES RUNGE KUTTA 4

```
subroutine fcn(t,y,v)
implicit real*8(a-h,o-z)
subroutine for wolf integration
dimension y(20),v(20)
common /params/ p,g
c generated by the REDUCE code
v(1)=y(3)
v(2)=y(4)
v(3)=(y(1)*(-2*y(2)**2-y(1)**2-2*g**2))/2
v(4)=y(2)*(-y(2)**2*p-y(1)**2-g**2+1)
v(5)=y(13)
v(6)=y(14)
v(7)=y(15)
v(8)=y(16)
v(9)=y(17)
v(10)=y(18)
v(11)=y(19)
v(12)=y(20)
v(13)=(-4*y(9)*y(2)*y(1)-2*y(5)*y(2)**2-3*y(5)*y(1)**2-2*y(5)*g . **2)/2
v(14)=(-4*y(10)*y(2)*y(1)-2*y(6)*y(2)**2-3*y(6)*y(1)**2-2*y(6)* . g**2)/2
v(15)=(-4*y(11)*y(2)*y(1)-2*y(7)*y(2)**2-3*y(7)*y(1)**2-2*y(7)* . g**2)/2
v(16)=(-4*y(12)*y(2)*y(1)-2*y(8)*y(2)**2-3*y(8)*y(1)**2-2*y(8)* . g**2)/2
v(17)=-3*y(9)*y(2)**2*p-y(9)*y(1)**2-y(9)*g**2+y(9)-2*y(5)*y(2) . *y(1)
v(18)=-3*y(10)*y(2)**2*p-y(10)*y(1)**2-y(10)*g**2+y(10)-2*y(6)* . y(2)*y(1)
v(19)=-3*y(11)*y(2)**2*p-y(11)*y(1)**2-y(11)*g**2+y(11)-2*y(7)* . y(2)*y(1)
v(20)=-3*y(12)*y(2)**2*p-y(12)*y(1)**2-y(12)*g**2+y(12)-2*y(8)* . y(2)*y(1)
return
end
```

SUBROUTINE

```
ODEINT(YSTART,NVAR,X1,X2,EPS,H1,HMIN,NOK,NBAD,DERIVS,RK *QC)
IMPLICIT REAL*8(A-H,O-Z)
PARAMETER (MAXSTP=10000,NMAX=20,TWO=2.0D0,ZERO=0.0D0,TINY=1.D-30)
COMMON /PATH/ KMAX,KOUNT,DXSAV,XP(200),YP(10,200)
DIMENSION YSTART(NVAR),YSCAL(NMAX),Y(NMAX),DYDX(NMAX)
X=X1
H=SIGN(H1,X2-X1)
NOK=0
NBAD=0
KOUNT=0
DO 11 I=1,NVAR
Y(I)=YSTART(I)
11 CONTINUE
XSAV=X-DXSAV*TWO
DO 16 NSTP=1,MAXSTP
CALL DERIVS(X,Y,DYDX)
DO 12 I=1,NVAR
YSCAL(I)=ABS(Y(I))+ABS(H*DYDX(I))+TINY
12 CONTINUE
IF(KMAX.GT.0)THEN
IF(ABS(X-XSAV).GT.ABS(DXSAV)) THEN
IF(KOUNT.LT.KMAX-1)THEN
KOUNT=KOUNT+1
XP(KOUNT)=X
DO 13 I=1,NVAR
YP(I,KOUNT)=Y(I)
13 CONTINUE
XSAV=X
ENDIF
ENDIF
ENDIF
```

```
IF((X+H-X2)*(X+H-X1).GT.ZERO) H=X2-X
CALL RKQC(Y,DYDX,NVAR,X,H,EPS,YSCAL,HDID,HNEXT,DERIVS)
IF(HDID.EQ.H)THEN
NOK=NOK+1
ELSE
NBAD=NBAD+1
ENDIF
IF((X-X2)*(X2-X1).GE.ZERO)THEN
DO 14 I=1,NVAR
YSTART(I)=Y(I)
14 CONTINUE
IF(KMAX.NE.0)THEN
KOUNT=KOUNT+1
XP(KOUNT)=X
DO 15 I=1,NVAR
YP(I,KOUNT)=Y(I)
15 CONTINUE
ENDIF
RETURN
ENDIF
IF(ABS(HNEXT).LT.HMIN) PAUSE 'Stepsize smaller than minimum.'
H=HNEXT
16 CONTINUE
PAUSE 'Too many steps.'
RETURN
END


SUBROUTINE RK4(Y,DYDX,N,X,H,YOUT,DERIVS)
implicit real*8(a-h,o-z)
PARAMETER (NMAX=20)
DIMENSION Y(N),DYDX(N),YOUT(N),YT(NMAX),DYT(NMAX),DYM(NMAX)
```

```
HH=H*0.5
H6=H/6.
XH=X+HH
DO 11 I=1,N
YT(I)=Y(I)+HH*DYDX(I)
11 CONTINUE
CALL DERIVS(XH,YT,DYT)
DO 12 I=1,N
YT(I)=Y(I)+HH*DYT(I)
12 CONTINUE
CALL DERIVS(XH,YT,DYM)
DO 13 I=1,N
YT(I)=Y(I)+H*DYM(I)
DYM(I)=DYT(I)+DYM(I)
13 CONTINUE
CALL DERIVS(X+H,YT,DYT)
DO 14 I=1,N
YOUT(I)=Y(I)+H6*(DYDX(I)+DYT(I)+2.*DYM(I))
14 CONTINUE
RETURN
END


SUBROUTINE RKQC(Y,DYDX,N,X,HTRY,EPS,YSCAL,HDID,HNEXT,DERIVS)
implicit real*8(a-h,o-z)
PARAMETER (NMAX=20,FCOR=.0666666667d0,
* ONE=1.d0,SAFETY=0.9d0,ERRCON=6.d-4)
EXTERNAL DERIVS
DIMENSION
Y(N),DYDX(N),YSCAL(N),YTEMP(NMAX),YSAV(NMAX),DYSAV(NMAX)
PGROW=-0.20d0
PSHRNK=-0.25d0
```

```
XSAV=X
DO 11 I=1,N
YSAV(I)=Y(I)
DYSAV(I)=DYDX(I)
11 CONTINUE
H=HTRY
1 HH=0.5*H
CALL RK4(YSAV,DYSAV,N,XSAV,HH,YTEMP,DERIVS)
X=XSAV+HH
CALL DERIVS(X,YTEMP,DYDX)
CALL RK4(YTEMP,DYDX,N,X,HH,Y,DERIVS)
X=XSAV+H
IF(X.EQ.XSAV)PAUSE 'Stepsize not significant in RKQC.'
CALL RK4(YSAV,DYSAV,N,XSAV,H,YTEMP,DERIVS)
ERRMAX=0.
DO 12 I=1,N
YTEMP(I)=Y(I)-YTEMP(I)
ERRMAX=MAX(ERRMAX,ABS(YTEMP(I)/YSCAL(I)))
12 CONTINUE
ERRMAX=ERRMAX/EPS
IF(ERRMAX.GT.ONE) THEN
H=SAFETY*H*(ERRMAX**PSHRNK)
GOTO 1
ELSE
HDID=H
IF(ERRMAX.GT.ERRCON)THEN
HNEXT=SAFETY*H*(ERRMAX**PGROW)
ELSE
HNEXT=4.d0*H
ENDIF
ENDIF
```

```
DO 13 I=1,N
Y(I)=Y(I)+YTEMP(I)*FCOR
13 CONTINUE
RETURN
END
```

APPENDIX D: MAPLE PROGRAM FOR LIE TRANSFORM METHOD

This Maple program uses Lie Transform algorithm for normalization of 2d- Hamiltonian with arbitrary frequencies w_1, w_2, and construct approximate integrals up to order 6.

```
with(DifferentialGeometry):
with(LieAlgebras):
DGsetup([x1,x2,y1,y2,M]):
w1:=1: w2:=1:
H:=1/2*w1*(p1**2+q1**2)+1/2*w2*(p2**2+q2**2)+e**2/(2*w1*w2)*q1**2*q2**2;
sys:=x1=1/sqrt(2)*(q1+I*p1),x2=1/sqrt(2)*(q2+I*p2),y1=I/sqrt(2)*(q1-
I*p1),y2=I/sqrt(2)*(q2-I*p2):
T:=solve(sys,q1,q2,p1,p2,'parametric'):
for i from 1 to 2 do
p[i]:=rhs(T[1,i]):
q[i]:=rhs(T[1,i+2]):
od:
p1:=p[1]; p2:=p[2]; q1:=q[1]; q2:=q[2];
Hex:=expand(H):
L:=evalDG(w1*x1*D-x1+w2*I*x2*D-x2-w1*y1*D-y1-w2*I*y2*D-y2);
readlib(mtaylor):
readlib(coeftayl):
Q:=mtaylor(sum(sum(sum(sum(c[j,k,l,m]*x1**j*x2**k*y1**l*y2**m,j=0..4)
,k=0..4),l=0..4),m=0..4),[x1,x2,y1,y2],5):
for j from 0 to 4 do
for k from 0 to 4 do
for l from 0 to 4 do
for m from 0 to 4 do
if j+k+l+m ¡ 4 then
```

```
Q:=subs(c[j,k,l,m]=0,Q)
fi;
od;
od;
od;
od;
Q1:=expand(LieDerivative(L,Q)):
T1:=Hex-Q1:
for j from 0 to 4 do
for k from 0 to 4 do
for l from 0 to 4 do
for m from 0 to 4 do
if j+k+l+m=4 then
c[j,k,l,m]:=solve( coeftayl(T1,[x1,x2,y1,y2]=[0,0,0,0],[j,k,l,m])=0, c[j,k,l,m]);
fi;
od;
od;
od;
od;
H21:=eval(T1):
H0:=mtaylor(H21,[x1,x2,y1,y2],3):
K21:=H21-H0:
H2:=Hex-H0;
for j from 0 to 4 do
for k from 0 to 4 do
for l from 0 to 4 do
for m from 0 to 4 do
if j+k+l+m=4 then
Q:=subs(c[j,k,l,m]=0,Q)
fi;
od;
```

```
od;
od;
od;
unassign('p1'); unassign('p2'); unassign('q1'); unassign('q2');
K2:=simplify(subs(x1=1/sqrt(2)*(q1+I*p1),x2=1/sqrt(2)*(q2+I*p2),y1=I/sqrt(2)*(q1-
I*p1),y2=I/sqrt(2)*(q2-I*p2),K21));
g21:=simplify(subs(x1=1/sqrt(2)*(q1+I*p1),x2=1/sqrt(2)*(q2+I*p2),y1=I/sqrt(2)*(q1-
I*p1),y2=I/sqrt(2)*(q2-I*p2),Q)):
g2:=expand(g21);
PB:=proc(f,g)
diff(f,x1)*diff(g,y1)-diff(f,y1)*diff(g,x1)+diff(f,x2)*diff(g,y2)- diff(f,y2)*diff(g,x2)
end:
PB1:=expand(simplify(PB(Q,H2))):
PB2:=expand(simplify(PB(Q,K21))):
PB3:=1/2*(PB1+PB2):
unassign('j','k','l','m'):
TT:=mtaylor(sum(sum(sum(sum(a[j,k,l,m]*x1**j*x2**k*y1**l*y2**m,j=0..6),k=0..6)
,l=0..6),m=0..6),[x1,x2,y1,y2],7):
for j from 0 to 6 do
for k from 0 to 6 do
for l from 0 to 6 do
for m from 0 to 6 do
if j+k+l+m ¡ 6 then
TT:=subs(a[j,k,l,m]=0,TT)
fi;
od;
od;
od;
od;
TT:
TT22:=expand(LieDerivative(L,TT)):
```

```
NT:=PB3-TT22:
for j from 0 to 6 do
for k from 0 to 6 do
for l from 0 to 6 do
for m from 0 to 6 do
if j+k+l+m=6 then
a[j,k,l,m]:=solve( coeftayl(NT,[x1,x2,y1,y2]=[0,0,0,0],[j,k,l,m])=0,
a[j,k,l,m]);
fi;
od;
od;
od;
od;
K41:=eval(NT):
K42:=simplify(subs(x1=1/sqrt(2)*(q1+I*p1),x2=1/sqrt(2)*(q2+I*p2),y1=I/sqrt(2)*(q1-
I*p1)
,y2=I/sqrt(2)*(q2-I*p2),K41)):
K4:=expand(K42);
for j from 0 to 6 do
for k from 0 to 6 do
for l from 0 to 6 do
for m from 0 to 6 do
if j+k+l+m=6 then
TT:=subs(a[j,k,l,m]=0,TT)
fi;
od;
od;
od;
od;
TT:
TT2:=simplify(subs(x1=1/sqrt(2)*(q1+I*p1),x2=1/sqrt(2)*(q2+I*p2),y1=I/sqrt(2)*(q1-
```

```
I*p1),y2=I/sqrt(2)*(q2-I*p2),TT)):
g4:=expand(TT2);
I0:=simplify(subs(x1=1/sqrt(2)*(q1+I*p1),x2=1/sqrt(2)*(q2+I*p2),y1=I/sqrt(2)*(q1-
I*p1),y2=I/sqrt(2)*(q2-I*p2),H0)):
I21:=H2-K21:
I2:=simplify(subs(x1=1/sqrt(2)*(q1+I*p1),x2=1/sqrt(2)*(q2+I*p2),y1=I/sqrt(2)*(q1-
I*p1),y2=I/sqrt(2)*(q2-I*p2),I21));
I3:=H2-I21:
PB44:=expand(simplify(PB(Q,I3))):
I41:=PB44-K41:
I42:=simplify(subs(x1=1/sqrt(2)*(q1+I*p1),x2=1/sqrt(2)*(q2+I*p2),y1=I/sqrt(2)*(q1-
I*p1),y2=I/sqrt(2)*(q2-I*p2),I41)):
I4:=expand(I42);
PB51:=expand(simplify(PB(Q,H0))):
PB52:=expand(simplify(PB(Q,PB51))):
PB53:=expand(simplify(PB(Q,PB52))):
PB61:=expand(simplify(PB(Q,H0))):
PB62:=expand(simplify(PB(TT,PB61))):
PB72:=expand(simplify(PB(Q,PB1))):
PB81:=expand(simplify(PB(TT,H2))):
Q16:=-Q1:
PB511:=expand(simplify(PB(Q,Q16))):
PB513:=expand(simplify(PB(Q,PB511))):
PB611:=expand(simplify(PB(TT,Q16))):
RH:=1/6*PB513+PB611+1/2*PB72+PB81:
unassign('j','k','l','m'):
BD:=mtaylor(sum(sum(sum(sum(b[j,k,l,m]*x1**j*x2**k*y1**l*y2**m,j=0..8),k=0..8),
l=0..8),m=0..8),[x1,x2,y1,y2],9):
for j from 0 to 8 do
for k from 0 to 8 do
for l from 0 to 8 do
```

```
for m from 0 to 8 do
if j+k+l+m ¡ 8 then
BD:=subs(b[j,k,l,m]=0,BD)
fi;
od;
od;
od;
od;
BD1:=expand(LieDerivative(L,BD)):
NT6:=RH-BD1:
for j from 0 to 8 do
for k from 0 to 8 do
for l from 0 to 8 do
for m from 0 to 8 do
if j+k+l+m=8 then
b[j,k,l,m]:=solve( coeftayl(NT6,[x1,x2,y1,y2]=[0,0,0,0],[j,k,l,m])=0, b[j,k,l,m]);
fi;
od;
od;
od;
od;
K61:=eval(NT6):
K62:=simplify(subs(x1=1/sqrt(2)*(q1+I*p1),x2=1/sqrt(2)*(q2+I*p2),
y1=I/sqrt(2)*(q1-I*p1),y2=I/sqrt(2)*(q2-I*p2),K61)):
K6:=expand(K62);
for j from 0 to 8 do
for k from 0 to 8 do
for l from 0 to 8 do
for m from 0 to 8 do
if j+k+l+m=8 then
BD:=subs(b[j,k,l,m]=0,BD)
```

```
fi;
od;
od;
od;
od;
BD2:=simplify(subs(x1=1/sqrt(2)*(q1+I*p1),x2=1/sqrt(2)*(q2+I*p2),y1=I/sqrt(2)*(q1-
I*p1),y2=I/sqrt(2)*(q2-I*p2),BD)):
g6:=expand(BD2);
PB46:=expand(simplify(PB(Q,PB44))):
PB45:=expand(simplify(PB(TT,I3))):
I46:=-I41:
PB111:=expand(simplify(PB(Q,I46))):
I611:=-K61+1/2*PB46+PB45+PB111:
I612:=simplify(subs(x1=1/sqrt(2)*(q1+I*p1),x2=1/sqrt(2)*(q2+I*p2),
y1=I/sqrt(2)*(q1-I*p1),y2=I/sqrt(2)*(q2-I*p2),I611)):
I6:=expand(I612);
save I0,I2,I4,I6, "C:/Users/Dell Xps/integrals1-1.m"
```